Theory of the magnetic field modulated geminate recombination of radical ion pairs in polar solvents: Application to the pyrene–N,N-dimethylaniline system

ARTICLE *in* THE JOURNAL OF CHEMICAL PHYSICS · JULY 1977

Impact Factor: 2.95 · DOI: 10.1063/1.434868

3 AUTHORS, INCLUDING:

Hans-Joachim Werner
Universität Stuttgart
284 PUBLICATIONS **25,843** CITATIONS

SEE PROFILE

Theory of the magnetic field modulated geminate recombination of radical ion pairs in polar solvents: Application to the pyrene–*N*,*N*-dimethylaniline system

H.-J. Werner, Z. Schulten, and K. Schulten

Max-Planck-Institut für biophysikalische Chemie, Abt. Spektroskopie, D-3400 Göttingen, Federal Republic of Germany
(Received 11 January 1977)

Pairs of radical ions generated in polar solvents by photoinduced electron transfer either recombine within a few nanoseconds or separate. The (geminate) recombination process is governed by a hyperfine-coupling-induced coherent motion of the unpaired electron spins which can be modulated by weak external magnetic fields. The process which also generates the well-known CIDNP and CIDEP effects is described theoretically by a stochastic Liouville equation comprising for realistic systems a large set of coupled diffusion equations. For the integration of these equations a finite-difference algorithm with space and time discretization is developed. By comparison with exact solutions of the Liouville equation for model systems, it is demonstrated that an approximate Liouville equation which entails only two coupled diffusion equations for singlet and triplet radical pairs, respectively, suffices to predict the geminate recombination yields accurately. The approximate Liouville equation is employed then to study on the basis of known hyperfine coupling constants, second-order recombination rate constants, diffusion coefficients, and dielectric constants, the solvent, temperature, concentration, and magnetic field dependence of the geminate (singlet and triplet) recombination yields for the system pyrene–*N*,*N*-dimethylaniline. The effect of deuteration upon the recombination yield and its magnetic field dependence is also studied. Furthermore, the influence of an exchange interaction acting at small separations of the radicals is investigated for a model system.

I. INTRODUCTION

Most chemical reactions proceed in liquid media and are strongly influenced by their solvent environment. To gain detailed information on reactions in solvents it is desirable to observe primary reaction encounters which encompass the reaction or final separation of a reactant pair after a multitude of binary collisions.

In the case of radical reactions, information about the encounter process can be conveyed by a coherent motion of the unpaired electron spins. This motion is induced by the hyperfine coupling between electron and nuclear spins and serves as an internal clock measuring the duration of the encounter as well as the reaction probabilities. The spin motion namely leaves its trace on the NMR signals of the nuclear spins of the products (CIDNP effect) and on the ESR signals of the electron spins of the escaped radicals (CIDEP effect).[1] Unfortunately, the NMR and ESR spectra are averaged over times much longer than the duration of single radical pair encounters and hence yield only limited information.

Recently, we succeeded to observe by means of nanosecond spectroscopy a magnetic field modulation on the initial (~ 10 ns) recombination yields of radical ion pairs which were generated through photoinduced electron transfer.[2,3] Although such observations appear to be more limited in their range of applicability than the CIDNP and CIDEP measurements they convey the most direct information on radical processes in liquids. In order to unveil this information a *quantitative* theory of the radical recombination process which links the generation, diffusion, spin motion, and recombination of the radical ion pairs will be given in this paper. We shall show that the observed solvent effects on the recombination yields and their magnetic field dependence can be rationalized in terms of well-known solvent–solute properties, viz., diffusion constants, dielectric constants, second-order recombination rate constants, and hyperfine coupling constants.

Let us first summarize the experimental findings which provide the basis for our theoretical study. Radical ion pairs (e.g., $^2Py^- + {}^2DMA^+$) can be generated in polar solvents via photoinduced electron transfer between suitable acceptor (^1Py) and donor (^1DMA) molecules (Py = pyrene, DMA = N_1N-dimethylaniline).[4] The radical ion pairs recombine to the ground state and, if energetically possible, to the triplet state of one of the neutral molecules.[2–7] Time-resolved experiments[2,3,5–7] show that the recombination takes place on two different time scales: either the original pairs recombine directly within a few nanoseconds by an *"intrapair"* or *"geminate"* process, or the pairs diffuse apart and recombine with members of other pairs in an *"interpair"* or *"homogeneous"* process. The latter reaction for typical radical ion pair concentrations takes place over the time range of some microseconds. The *interpair* encounters occur with a random spin alignment, i.e., 75% are in a triplet and 25% in a singlet electron spin state initially. Thus, the observation of triplet product formation in the slow *homogeneous* phase of the reaction is readily explained. However, triplet products are also observed in the fast *geminate* phase of the recombination process.[2,3,5,7] Since the radical ion pairs are generated from singlet precursors, their unpaired electron spins are aligned in a singlet state initially. Consequently, there must exist a mechanism by which the electron spin multiplicity is changed within a few nanoseconds.

As suggested by Groff *et al.*[8] and Brocklehurst,[9] the *hyperfine coupling* between the unpaired electron spins

and the nuclear spins should be able to induce the fast spin multiplicity change of the electron spin state during the geminate phase of the recombination process. Since the hyperfine coupling is extremely weak ($\sim 10^{-6}$ eV), this mechanism is expected to be only effective in "solvent-shared" radical ion pairs, in which the singlet and triplet electron spin states are degenerate. The degeneracy between the S, T_0 and $T_{\pm 1}$ states is lifted, however, if an external magnetic field is applied to the system. For (Zeeman) energy splittings of the order of the hyperfine coupling energy the $S, T_0 - T_{\pm 1}$ transition probabilities will be reduced and will vanish in the presence of large fields ($\gtrsim 200$ G). Thus a lowering of the geminate triplet recombination yield is to be expected when a magnetic field is applied. As a magnetic field effect should not arise for the homogeneous recombination (see Ref. 2 and Sec. VI of this paper) or for intersystem crossing in a possible intermediate charge transfer complex (in which the singlet and triplet states are not degenerate) preceding the ion pair formation, *the magnetic field effect separates out the geminate recombination process.*

We recently succeeded in observing such a magnetic field modulation of the triplet recombination yield for the system pyrene–3,5-dimethoxy-*N*,*N*-dimethylaniline (Py–DMDMA) in methanol.[2] A time-resolved experiment proved that the magnetic field effect builds up during the geminate phase of the recombination process. Furthermore, the magnetic field dependence of the observed triplet recombination yield was found to be in excellent agreement with the predictions of a theoretical model based on the hyperfine mechanism. In this model the separation and recombination of the radical ion pairs were described by a simple first-order kinetic reaction scheme. A rather similar model has recently been published by Michel-Beyerle *et al.*[10] We would like to note, however, that such a kinetic model gives unreasonable triplet yields in the case of different singlet and triplet recombination rate constants, a shortcoming which has already been demonstrated and corrected in Ref. 2.

Clearly, a realistic treatment of the geminate recombination process has to take into account the relative diffusion of the radical ion pair described by a pair distribution function. For this purpose a numerical calculation of the radical ion pair distribution function was carried out, and on the basis of a simple two-proton radical ion pair model system, the qualitative features of the geminate recombination process could be explained in terms of solvent properties.[11] The recombination was assumed to be spin independent, i.e., to occur with equal probability for singlet and triplet pairs. However, as we will show below, this assumption is not justified in general. In order to obtain *quantitative* predictions about the radical ion pair diffusion and recombination and to render possible a direct comparison between experiment and theory we will in this paper extend the theory of the hyperfine-induced geminate recombination to realistic systems. We choose as an example the $^2Py^- + {}^2DMA^+$ radical ion pair which also has been the subject of experimental investigations.[3] This will be done here unaffected by the criticism of Michel-Beyerle *et al.*,[10] who advocated an oversimplified first-order kinetic treatment of the geminate process dispensing from any quantitative analysis of experimental observations.

For a quantitative description of the hyperfine-induced geminate triplet formation it is of cardinal importance to account correctly for the time evolution of the singlet-triplet transition probability which in the case of the $^2Py^- + {}^2DMA^+$ system is due to the hyperfine coupling of the two unpaired electrons to 22 nuclear spins. The geminate recombination yields depend also crucially on the reaction probabilities of the radical ion pair in the singlet and triplet states. We will show that these probabilities can be determined from observed second-order (homogeneous) recombination rate constants. It turns out that the singlet and triplet recombination probabilities are rather different. This leads to a coupling between the solvent-governed diffusion and the spin motion and recombination, i.e., the radical ion pairs have to be described by a large set of coupled diffusion equations.

In Sec. II we introduce the stochastic Liouville equation accounting for the radical ion pair diffusion, spin motion, and recombination. In Sec. III we present a numerical algorithm to evaluate the time evolution of the electron spin states of radical pairs in which the electrons are coupled to a large number of nuclear spins. In Sec. IV we furnish numerical (finite-difference) methods for the solution of the stochastic Liouville equation and supply tests for their accuracy. In Sec. V we investigate the effect of the exchange interaction in the contact region of the radical pairs. In Sec. VI we provide the connection between the geminate recombination rate constants and the observed second-order (homogeneous) recombination rate constants. Finally, in Sec. VII we apply the theory to the system $^2Py^- + {}^2DMA^+$ and investigate the effects of the solvent, temperature, magnetic field, concentration, and deuteration on the geminate recombination yields.

II. THE STOCHASTIC LIOUVILLE EQUATION FOR RECOMBINING RADICAL PAIRS

The generation, diffusion, spin motion, and recombination of radical pairs is described by the density matrix $\rho(r,t)$, which is the solution of the stochastic Liouville equation

$$\frac{\partial}{\partial t}\rho(r,t) = R(t)\frac{\delta(r-r_1)}{4\pi r_1^2 Z}\,Q_s + l(r)\rho(r,t) - \frac{i}{\hbar}[H,\rho(r,t)]_- - \tfrac{1}{2}s(r)\{\kappa_S[Q_S,\rho(r,t)]_+ + \kappa_T[Q_T,\rho(r,t)]_+\} - k_{\mathrm{rec}}\langle\rho(t)\rangle\rho(r,t)\,, \tag{2.1a}$$

$$\rho(r,0) \equiv 0\,, \tag{2.1b}$$

where $[A,B]_{\pm}=AB\pm BA$. This equation implies the radical ion pair generation and recombination to be independent of the relative orientation of the radicals and $\rho(r,t)$ to be spherically symmetric. The diagonal elements $4\pi r^2\rho_{ii}(r,t)dr$ represent the concentration of pairs in the volume element $4\pi r^2\,dr$ in some electron–nuclear spin state $|i\rangle$ at time t. The total concentration of pairs is $\langle\rho(t)\rangle=4\pi\int_{r_1}^{\infty}r^2\,\mathrm{Tr}\rho(r,t)\,dr$, where $\mathrm{Tr}A=\sum_i A_{ii}$.

The first term on the rhs of Eq. (2.1) describes the generation of the radical pairs which are assumed to be formed at the distance $r=r_1$ in the singlet electron spin state with equal probability for all Z nuclear spin states ($Z=\mathrm{Tr}Q_S$).

The rate of formation $R(t)$ is defined to yield the total concentration of pairs generated,

$$\int_0^{\infty}R(t)\,dt=c_0\,. \tag{2.2}$$

The second term of Eq. (2.1) describes the relative diffusion of the radical pair. $l(r)$ is the Smoluchowski operator

$$l(r)=D\left\{\frac{1}{r}\frac{\partial^2}{\partial r^2}r-\beta\frac{1}{r^2}\left[\frac{\partial}{\partial r}r^2F(r)\right]-\beta F(r)\frac{\partial}{\partial r}\right\}, \tag{2.3}$$

where $\beta=1/kT$, and $D=D_1+D_2$ is the sum of the diffusion coefficients of the two radicals. $F(r)$ is the radial force acting between the radicals, e.g., $F(r)=0$ for neutral molecules (free diffusion) or $F(r)=-e^2/\epsilon r^2$ for a radical ion pair $^2A^{-}+{}^2D^{+}$, where ϵ is taken to be the *macroscopic* dielectric constant of the medium. This description for the force field between radical ions holds strictly only at large distances and low ion concentrations. A more accurate representation of the force field between diffusing ions would need to include dynamic effects and a r dependence of the microscopic dielectric constant describing the solvent-screened Coulomb field over molecular distances.

The third term of Eq. (2.1) describes the electron–nuclear spin motion of the radical pair governed by the Hamiltonian

$$H(r)=\sum_k a_{1k}\mathbf{S}_1\cdot\mathbf{I}_k+\sum_l a_{2l}\mathbf{S}_2\cdot\mathbf{I}_l + \mu\mathbf{B}\cdot[g_1\mathbf{S}_1+g_2\mathbf{S}_2]-J(r)[\tfrac{1}{2}+2\mathbf{S}_1\cdot\mathbf{S}_2]\,. \tag{2.4}$$

The first and second terms in Eq. (2.4) represent the hyperfine interaction between the unpaired electron spins $\mathbf{S}_1$ and $\mathbf{S}_2$ and the nuclear spins $\mathbf{I}_k$, $\mathbf{I}_l$. The third (electron Zeeman) term accounts for the interaction between the electron spins and the applied magnetic field, and in the last term enters the exchange interaction $J(r)$ between the unpaired electron spins [singlet–triplet splitting $2J(r)$]. In the Hamiltonian we have neglected the smaller Zeeman terms and also all anisotropic terms as the radicals are assumed to be freely rotating in the solvent.

The fourth and fifth terms of Eq. (2.1) describe the geminate recombination to the singlet and triplet states, respectively. It is assumed that within the reaction domain $s(r)$ the singlet and triplet radical ion pairs undergo first-order recombination reactions with rate constants $s(r)\kappa_S$ and $s(r)\kappa_T$, respectively. Q_S and Q_T are the projection operators onto the manifold of singlet and triplet radical pair states. The reaction domain $s(r)$ will be normalized as $\int_{r_1}^{\infty}(r/r_1)^2s(r)\,dr=1$. This normalization ensures that for a *constant* distribution of radical pairs a variation of $s(r)$ does not lead to a variation of the reaction yield.

The last term of Eq. (2.1) represents the homogeneous recombination of the radical ion pairs. k_{rec} is the bimolecular recombination rate constant, which will be discussed in detail in Sec. VI.

The density matrix $\rho(r,t)$ can be factored into a scalar function $c(t)$, describing the depletion of the radical concentration through the homogeneous recombination, times a matrix $p(r,t)$ describing the time evolution of an isolated radical pair:

$$\rho(r,t)=c(t)\,p(r,t)\,, \tag{2.5}$$

$$\dot{c}(t)=-k_{\mathrm{rec}}\,c(t)^2\langle p(t)\rangle\,, \tag{2.6a}$$

$$c(0)=c_0\,, \tag{2.6b}$$

$$\frac{\partial}{\partial t}p(r,t)=R(t)\frac{\delta(r-r_1)}{4\pi r_1^2c_0Z}Q_S+l(r)p(r,t)-\frac{i}{\hbar}[H(r),p(r,t)]_- -\tfrac{1}{2}s(r)\{\kappa_S[Q_S,p(r,t)]_+ +\kappa_T[Q_T,p(r,t)]_+\}\,, \tag{2.7}$$

In this separation we assume $[c_0-c(t)]R(t)\simeq 0$, which is justified since $c(t)\simeq c_0$ during the short time of pair generation. Equation (2.6) has the solution

$$c(t)=c_0\left(1+k_{\mathrm{rec}}\,c_0\int_0^t\langle p(\tau)\rangle\,d\tau\right)^{-1}. \tag{2.8}$$

In order to solve Eq. (2.7) one may define $p(r,t)$ through the time convolution of $R(t)$ with a function $P(r,t)$

$$p(r,t)=\int_0^t R(\tau)P(r,t-\tau)\,d\tau\,, \tag{2.9}$$

where $P(r,t)$ describes an isolated radical pair generated at the instance $t=0$:

$$\frac{\partial}{\partial t}P(r,t)=l(r)P(r,t)-\frac{i}{\hbar}[H(r),P(r,t)]_- -\tfrac{1}{2}s(r)\{\kappa_S[Q_S,P(r,t)]_+ +\kappa_T[Q_T,P(r,t)]_+\}\,, \tag{2.10a}$$

$$P(r,0)=Q_S\delta(r-r_1)/(4\pi r_1^2c_0Z)\,. \tag{2.10b}$$

The Liouville equation (2.10) couples the diffusive motion, the recombination process, and the electron–nuclear spin motion of a radical pair. It cannot be simplified further except in the case of zero exchange interaction and identical singlet and triplet recombination rate constants κ_S and κ_T, respectively. For this case one may factor the solution of Eq. (2.10),

$$P(r,t)=d(r,t)P^0(t)\,, \tag{2.11}$$

where $d(r,t)$ is the scalar pair distribution function satisfying the diffusion equation ($\kappa_S=\kappa_T=\kappa$)

$$\frac{\partial}{\partial t} d(r,t) = [l(r) - \kappa s(r)]\, d(r,t) \,, \tag{2.12a}$$

$$d(r,0) = \delta(r - r_1)/(4\pi r_1^2 c_0) \,, \tag{2.12b}$$

and where $P^0(t)$ represents the electron–nuclear spin-density matrix of the radical pair which is the solution of the Liouville equation

$$\dot{P}^0(t) = -\frac{i}{\hbar}[H, P^0(t)]_- \tag{2.13a}$$

with the initial condition

$$P^0(0) = Q_S/Z \,. \tag{2.13b}$$

$p_S^0(t) = \mathrm{Tr}[Q_S P^0(t)]$ is the probability to find a radical pair in the singlet electron spin state at time t, disregarding the depletion of radicals through recombination which is accounted for in Eq. (2.12a). $p_T^0(t) = 1 - p_S^0(t)$ gives the probability of finding the pair in a triplet state.

The rates of recombination to singlet and triplet products are

$$\dot{n}_{S,T}(t) = \kappa p_{S,T}^0(t) \int_{r_1}^{\infty} 4\pi r^2 s(r)\, d(r,t)\, dr \,, \tag{2.14}$$

i.e., they are proportional to the number of radical pairs in the reaction domain defined through $s(r)$ and to the probability $p_S^0(t)[p_T^0(t)]$ to find the pair in a singlet [triplet] electron spin state at the instance of recombination. In Ref. 11 the exact solution of the Liouville equation (2.13) for the electron–nuclear spin motion of a very simple radical pair system was given along with a finite-difference evaluation of the pair distribution function $d(r,t)$. In Sec. III of this paper we will furnish the numerical solution of (2.13) for real radical pair systems with a large number of nuclear spins coupled to the unpaired electron spins.

For the case of unequal singlet and triplet recombination rate constants κ_S and κ_T, respectively, the separation of the diffusive motion and the spin motion of the radical pairs is not possible. The stochastic Liouville equation (2.10a) then comprises a large set of coupled diffusion equations for each element of the density matrix $P_{ij}(r,t)$, the indices i,j corresponding to electron–nuclear spin states. In the following we assume a basis in which the two unpaired electron spins are coupled to singlet and triplet states:

$$\text{Singlet:} \quad |S,N\rangle = 2^{-1/2}(|\alpha\beta,N\rangle - |\beta\alpha,N\rangle) \,,$$

$$\text{Triplet:} \quad |T_0,N\rangle = 2^{-1/2}(|\alpha\beta,N\rangle + |\beta\alpha,N\rangle) \,,$$

$$|T_1,N\rangle = |\alpha\alpha,N\rangle \,,$$

$$|T_{-1},N\rangle = |\beta\beta,N\rangle \,,$$

where $|\sigma_1\sigma_2,N\rangle$ denotes an electron–nuclear spin state with electron spin $\sigma_1(\sigma_2)$ on radical 1(2) and nuclear spin state $|N\rangle$. For a numerical solution of (2.10) one may separate the real and imaginary parts $R_{ij} = \mathrm{Re}[P_{ij}(r,t)]$ and $S_{ij} = \mathrm{Im}[P_{ij}(r,t)]$ to obtain the coupled equations

$$\frac{\partial}{\partial t} R_{ij} = \frac{1}{\hbar}\Big(\sum_{k\neq i,j}(H_{ik}S_{kj} + H_{jk}S_{ki}) + [H_{ii}(r) - H_{jj}(r)]S_{ij}\Big) + [l(r) - U_{ii}(r) - U_{jj}(r)]R_{ij} \,, \tag{2.15a}$$

$$\frac{\partial}{\partial t} S_{ij} = -\frac{1}{\hbar}\Big(\sum_{k\neq i} H_{ik}R_{kj} - \sum_{k\neq j} H_{jk}R_{ki} + [H_{ii}(r) - H_{jj}(r)]R_{ij}\Big) + [l(r) - U_{ii}(r) - U_{jj}(r)]S_{ij} \,. \tag{2.15b}$$

The r dependence of the diagonal elements $H_{ii}(r)$ of the spin Hamiltonian is due to the exchange interaction $J(r)$. $U_{ii}(r)$ are the elements of the diagonal matrix $\frac{1}{2}s(r)(\kappa_S Q_S + \kappa_T Q_T)$, describing the recombination to singlet and triplet products. The corresponding recombination rates are

$$\dot{n}_{S,T}(t) = \kappa_{S,T} \int_{r_1}^{\infty} 4\pi r^2\, s(r) \sum_i Q_{S,T}^{ii} R_{ii}(r,t)\, dr \,. \tag{2.15c}$$

The number of electron–nuclear spin states $|i\rangle$ for the radical pair systems studied experimentally[2,3] is very large. In general, the solution of (2.15) is possible only for radical pairs containing just a few nuclear spins except at very high magnetic fields in which limit all nuclear spin states are independent. For a system containing two $\frac{1}{2}$ nuclear spins Eq. (2.15) will be solved for arbitrary magnetic fields in Sec. IV. There Eq. (2.15) will be integrated also for high ($B \to \infty$) magnetic fields for the system $^2\mathrm{Py}^- + {}^2\mathrm{DMA}^+$.

We will now derive an approximation to the Liouville equation (2.10) which renders possible a solution for radical pair systems of realistic complexity. This approximation will neglect the exchange interaction $J(r)$, which is expected to be rapidly decreasing with increasing pair separation. [The influence of $J(r)$ on the radical ion pair recombination process will be studied in Sec. V.] As already discussed in Ref. 2, the effect of different recombination rate constants κ_S and κ_T is to alter the electron–nuclear spin motion of the radical pairs in the reaction domain. The overall influence of this effect should be small for the spin motion of freely diffusing radicals or radical ions $^2\mathrm{A}^- + {}^2\mathrm{D}^+$ in rather polar solvents like acetonitrile or methanol but could become important in the case of stronger Coulomb attraction in less polar solvents such as propanol. For a radical pair initially in the singlet electron spin state and nuclear spin state $|N\rangle$ the exact Liouville equation is

$$\frac{\partial}{\partial t} P_N(r,t) = l(r) P_N(r,t) - \frac{i}{\hbar}[H, P_N(r,t)]_- - \tfrac{1}{2}s(r)\{\kappa_S[Q_S, P_N(r,t)]_+ + \kappa_T[Q_T, P_N(r,t)]_+\} \,, \tag{2.16a}$$

$$P_N(r,0) = \frac{\delta(r - r_1)}{4\pi r_1^2 c_0} |S,N\rangle\langle S,N| \,. \tag{2.16b}$$

Neglecting the effect of $\kappa_S \neq \kappa_T$ on the spin motion of the radical pair implies the factorization $P_N(r,t) = P_N^0(t)\,\mathrm{Tr}[P_N(r,t)]$. This may be introduced into the second term of Eq. (2.16a), i.e., $[H, P_N(r,t)]_- \simeq [H, P_N^0(t)]_- \mathrm{Tr} P_N(r,t)$, where $P_N^0(t)$ is the spin density matrix of the pair without reaction as defined through Eq. (2.13a) with the initial condition $P_N^0(0) = |S,N\rangle\langle S,N|$. For the total densities $p_{NS}(r,t) = \mathrm{Tr}[Q_S P_N(r,t)]$ and $p_{NT}(r,t) = \mathrm{Tr}[Q_T P_N(r,t)]$ of singlet and triplet pairs, respectively, follow the coupled equations $\{p_{NS}^0(t) = \mathrm{Tr}[Q_S P_N^0(t)];\ p_{NT}^0(t) = \mathrm{Tr}[Q_T P_N^0(t)]\}$

$$\frac{\partial}{\partial t} p_{NS}(r,t) = [l(r) - \kappa_S s(r)] p_{NS}(r,t) + \dot{p}^0_{NS}(t)[p_{NS}(r,t) + p_{NT}(r,t)] , \quad (2.17a)$$

$$\frac{\partial}{\partial t} p_{NT}(r,t) = [l(r) - \kappa_T s(r)] p_{NT}(r,t) + \dot{p}^0_{NT}(t)[p_{NS}(r,t) + p_{NT}(r,t)] . \quad (2.17b)$$

In a second step we average over all nuclear spin states N and introduce the approximations [note $p^0_S(t) = (1/Z) \times \sum_N p^0_{NS}(t)$]

$$\sum_N \dot{p}^0_{NS}(t)[p_{NS}(r,t) + p_{NT}(r,t)] \simeq \dot{p}^0_S(t) \sum_N [p_{NS}(r,t) + p_{NT}(r,t)] , \quad (2.18a)$$

$$\sum_N \dot{p}^0_{NT}(t)[p_{NS}(r,t) + p_{NT}(r,t)] \simeq \dot{p}^0_T(t) \sum_N [p_{NS}(r,t) + p_{NT}(r,t)] . \quad (2.18b)$$

We then obtain for the mean concentration of singlet and triplet pairs $p_S(r,t) = (1/Z)\sum_N p_{NS}(r,t)$ and $p_T(r,t) = (1/Z) \times \sum_N p_{NT}(r,t)$, respectively, the coupled equations

$$\frac{\partial}{\partial t} p_S(r,t) \simeq [l(r) - \kappa_S s(r)] p_S(r,t) + \dot{p}^0_S(t)[p_S(r,t) + p_T(r,t)] , \quad (2.19a)$$

$$\frac{\partial}{\partial t} p_T(r,t) \simeq [l(r) - \kappa_T s(r)] p_T(r,t) + \dot{p}^0_T(t)[p_S(r,t) + p_T(r,t)] . \quad (2.19b)$$

For the case $\kappa_S = \kappa_T$ these equations are exact. The recombination rates to the singlet and triplet products are

$$\dot{n}_{S,T}(t) = \kappa_{S,T} \int_{r_1}^{\infty} 4\pi r^2 s(r) p_{S,T}(r,t)\, dr . \quad (2.19c)$$

For simple radical pair systems with a small number of nuclear spins coupled to the unpaired electron spins, $p^0_T(t)$ is a simple periodic function which vanishes at $t = 0$ and reaches the value zero again after a relatively short time. In the case $\kappa_S = \kappa_T$ the triplet probability $p_T(r,t)$ and its time derivative $\dot{p}_T(r,t)$ vanish simultaneously. However, in the case $\kappa_T > \kappa_S$ the triplet probability $p_T(r,t)$, as evaluated from Eq. (2.19), reaches zero earlier than $p^0_T(t)$. At this instance $\dot{p}^0_T(t)$ and, thus, $\dot{p}_T(r,t)$ is still negative and therefore small negative values for $p_T(r,t)$ can be obtained over short time intervals. To avoid this defect of the approximation (2.19) we set $\dot{p}_{S,T}(r,t)$ to zero if $p_{S,T}(r,t) = 0$ and $\dot{p}^0_{S,T}(t) < 0$ in the numerical treatment (see Sec. IV). However, for radical pair systems which carry a large number of nuclear spins coupled to the unpaired electron spins, as for instance pyrene–DMA, the first zero point of $p^0_T(t)$ is reached only after times very long in comparison with the geminate phase of the recombination processes and, hence, the defect discussed does not occur for such systems.

In Sec. IV a numerical method for the solution of Eqs. (2.6), (2.15), and (2.19) will be presented, and it will be demonstrated that the singlet and triplet recombination yields

$$\phi^{\text{gem}}_{S,T}(t) = \int_0^t \dot{n}_{S,T}(\tau)\, d\tau \quad (2.20)$$

as determined from (2.19) are in excellent agreement with the results of the exact Liouville equation (2.15). The equation (2.19) will serve in Sec. VII to study the solvent and temperature effects on the geminate recombination of the $^2Py^- + {}^2DMA^+$ radical ion pair system.

III. HYPERFINE COUPLING INDUCED SINGLET ⇔ TRIPLET TRANSITION PROBABILITIES OF RADICAL PAIRS

We present now a numerical method for the evaluation of the time-dependent triplet probability $p^0_T(t)$ for radical ion pair systems with a large number of nuclear spins. The method was already employed in Ref. 2 and will be applied here to the system pyrene–N,N-dimethylaniline. The triplet probability has been defined in Sec. II to be $p^0_T(t) = \mathrm{Tr}[Q_S P^0(t)]$, where $P^0(t)$ is the electron–nuclear spin density matrix that satisfies the Liouville equation (2.13). The formal solution of (2.13) is

$$P^0(t) = \frac{1}{Z} \exp\left(-\frac{i}{\hbar} Ht\right) Q_S \exp\left(\frac{i}{\hbar} Ht\right) , \quad (3.1)$$

where H is the Hamiltonian defined in (2.4) with the exchange interaction $J(r) = 0$. This expression assumes that initially ($t = 0$) all Z nuclear spin states are equally populated in the *singlet* electron spin state. Expanding the evolution operator $\exp[-(i/\hbar)Ht]$ in terms of the eigenstates $|I\rangle$ of the Hamiltonian H ($H|I\rangle = E_I|I\rangle$), one derives for the singlet probability $p^0_S(t)$ the expression

$$p^0_S(t) = \frac{1}{Z} \mathrm{Tr}\left[Q_S \exp\left(-\frac{i}{\hbar} Ht\right) Q_S \exp\left(\frac{i}{\hbar} Ht\right)\right] = \frac{1}{Z}\sum_I \langle I|Q_S|I\rangle^2 + \frac{2}{Z}\sum_{I<J} \cos(\omega_{IJ}t)\,|\langle I|Q_S|J\rangle|^2 , \quad (3.2)$$

where

$$\omega_{IJ} = (E_I - E_J)/\hbar .$$

By virtue of

$$2\sum_{I<J} |\langle I|Q_S|J\rangle|^2 = Z - \sum_I \langle I|Q_S|I\rangle^2 \quad (3.3)$$

follows from (3.2)

$$p^0_S(t) = 1 - \frac{2}{Z}\sum_{I<J} (1 - \cos\omega_{IJ}t)\,|\langle I|Q_S|J\rangle^2 = 1 - \frac{2}{Z}\sum_{I<J}\left[(1 - \cos\omega_{IJ}t)\left(\sum_N \langle I|S,N\rangle\langle S,N|J\rangle\right)^2\right] . \quad (3.4)$$

If the radical ion pairs are initially formed in a *triplet* state, the transition probability to the singlet state $p^0_{T\to S}$ is $\frac{1}{3}$ of the transition probability $p^0_T(t)$ from the singlet to the triplet state:

$$p^0_{T\to S}(t) = \frac{1}{3Z}\mathrm{Tr}\left[Q_S \exp\left(-\frac{i}{\hbar} Ht\right) Q_T \exp\left(\frac{i}{\hbar} Ht\right)\right] = \frac{1}{3}\left\{1 - \frac{1}{Z}\mathrm{Tr}\left[Q_S \exp\left(-\frac{i}{\hbar} Ht\right) Q_S \exp\left(\frac{i}{\hbar} Ht\right)\right]\right\}$$

or

$$p^0_{T\to S}(t) = \tfrac{1}{3}[1 - p^0_S(t)] . \quad (3.5)$$

Since the exchange interaction between the radicals is neglected, the eigenstates of the Hamiltonian can be obtained as the direct product of the eigenstates of the two spin Hamiltonians H_1 and H_2,

$$H_i = g_i \mu B S_i^z + \sum_k^{(i)} a_{ik}[I_k^z S_i^z + \tfrac{1}{2}(S_i^+ I_k^- + S_i^- I_k^+)] \qquad (3.6)$$

of the separated radicals. S^z and I^z are the operators measuring the z components of the electron and nuclear spins, respectively, and $S^\pm$, $I^\pm$ are the corresponding shift operators. The summation in Eq. (3.6) is restricted to the nuclei k at radical i. The eigenvectors of $H_1 + H_2$ are first determined in the basis $|\sigma_1\sigma_2, N\rangle = |\sigma_1 N_1\rangle |\sigma_2 N_2\rangle$, where σ_i denotes the electron spin direction (α or β) and N_i the nuclear spin configuration on radical i. The eigenvectors in the coupled electron spin basis $|S, N\rangle$, $|T_0, N\rangle$, $|T_{\pm 1}, N\rangle$ and in the decoupled electron spin basis $|\sigma_1\sigma_2, N\rangle$ are connected through

$$\langle S, N|I\rangle = \frac{1}{\sqrt{2}}(\langle \alpha\beta, N|I\rangle - \langle \beta\alpha, N|I\rangle) ,$$

$$\langle T_0, N|I\rangle = \frac{1}{\sqrt{2}}(\langle \alpha\beta, N|I\rangle + \langle \beta\alpha, N|I\rangle) ,$$

$$\langle T_1, N|I\rangle = \langle \alpha\alpha, N|I\rangle ,$$

$$\langle T_{-1}, N|I\rangle = \langle \beta\beta, N|I\rangle . \qquad (3.7)$$

It is obvious that the Hamiltonian H_i of Eq. (3.6) is block diagonal with respect to the total z component of the electron–nuclear spin states. Further simplification can be achieved by coupling together the spins of nuclei with equal hyperfine constants on each radical into pseudo spin states characterized by the quantum numbers J, M. For N equivalent nuclei ($N > 2$) coupled together, in general more than one spin eigenfunction corresponds to a given J, M state. In the case that all nuclei have spin $\frac{1}{2}$, the number n_J of linearly independent spin functions for each J, M is given by the formula[12]

$$n_J = \binom{N}{\frac{N}{2} - J} - \binom{N}{\frac{N}{2} - J - 1} \qquad (3.8)$$

If there are m sets of equivalent nuclei each possible set of J values $(J_1, J_2, \ldots, J_m)$ gives rise to $\Pi_{i=1}^m n_{J_i}$ identical blocks in the Hamiltonian. This lowers to a large extent the number of the nuclear spin states to be considered explicitly. Also the block dimensions which determine crucially the numerical effort for the evaluation of the sums in Eq. (3.4) are reduced considerably if equivalent nuclei are coupled together. Nevertheless, for real systems the summations in (3.4) are over numerous states and the evaluation of p_S^0 requires a great computational effort. For instance, for the system pyrene–DMA discussed below the total number of electron–nuclear spin states to be taken into account is 1 572 864. Only 46 600 of these states are not degenerate. In the decoupled basis $|\sigma_1\sigma_2' N\rangle$ the Hamiltonian decomposes into 4320 blocks, the largest with dimension 72. Because of additional symmetry in the Hamiltonian (conservation of total spin) the computation is simplified for vanishing magnetic field B. The numerical accuracy of the results has been tested for the high field case ($B \to \infty$) by comparison with results obtained by means of the simple analytical expression (A3) derived by Brocklehurst[9] (see Appendix). The absolute accuracy was found to be better than 10^{-4}.

In order to reduce the computational effort for the evaluation of $p_T^0(t)$ and its time derivative $\dot{p}_T^0(t)$ for the system pyrene–DMA, which has been studied experimentally, we approximate the actual set of hyperfine coupling constants of pyrene[13] (in gauss)

$$4x(a_H = 2.13); \quad 4x(a_H = 4.83); \quad 2x(a_H = 1.04)$$

by the smaller set

$$4x(a_H = 2.3); \quad 4x(a_H = 5.2) . \qquad (3.9)$$

This replacement leaves the total sum of the hyperfine constants invariant. As is shown in the Appendix for the high field case, this invariance leaves essentially unaltered the fast initial rise of the triplet probability $p_T^0(t)$ on which the recombination yield depends most crucially.

Unfortunately, the hyperfine constants of DMA are not known. We assume that they are close to those of N, N-dimethyl-toluidine[14] if one takes the coupling constants of the para proton identical to those of the ortho protons. Again we replace the set of hyperfine coupling constants thus obtained,

$$6x(a_{CH_3} = 12.22); \quad 1x(a_N = 11.17);$$

$$3x(a_H = 5.21); \quad 2x(a_H = 1.36) ,$$

by the smaller set

$$6x(a_{CH_3} = 12.0); \quad 1x(a_N = 12.0); \quad 3x(a_H = 6.25), \qquad (3.10)$$

leaving the sum of coupling constants on the ^{2}DMA$^\cdot$ radical invariant.

Figure 1 presents the time evolution of the triplet probability $p_T^0(t)$ of the system ^{2}Py$^-$ + ^{2}DMA$^\cdot$ for various magnetic field strengths. The radical pairs are initially all in the singlet electron spin state, i.e., $p_T^0(0) = 0$. In Fig. 1 one can see that after a sharp rise during the first 5 ns the triplet probability assumes roughly a constant value which depends on the field strength. At long times and zero magnetic field approximately 70% of the radical pairs are in a triplet state. For large fields the

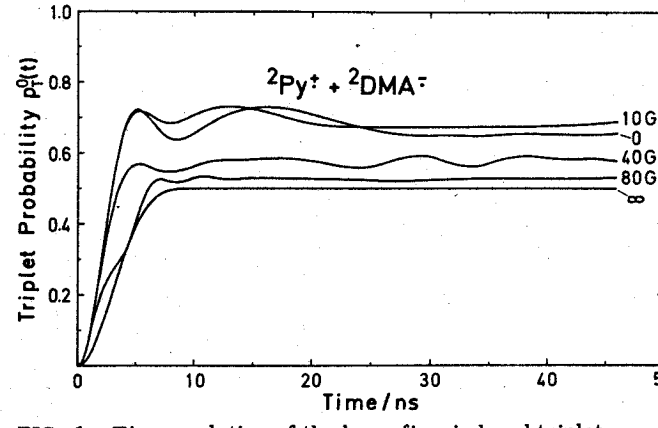

FIG. 1. Time evolution of the hyperfine-induced triplet probability $p_T^0(t)$ for the radical pair system ^{2}Py$^-$ + ^{2}DMA$^\cdot$ for magnetic fields $B = 0$, 10, 40, 80 G and $B \to \infty$. The hyperfine coupling constants are given in the text.

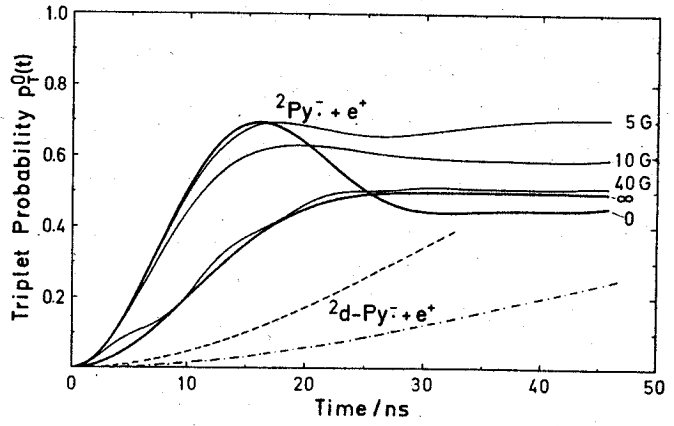

FIG. 2. Time evolution of the triplet probability $p_T^0(t)$ for the radical pair systems $^2Py^- + e^+$ and ^2d-$Py^- + e^+$ (see text) for various field strengths. – – –: ^2d-$Py^- + e^+$, $B = 0$; – · – · –: ^2d-$Py^- + e^+$, $B \to \infty$.

$T_{\pm 1}$ triplet states are decoupled from the S, T_0 states and only 50% of the radical pairs are found in the triplet state at long times. The triplet probabilities in Fig. 1 provide the necessary information on the spin motion of the radical pairs which will be needed later on to solve the stochastic Liouville equation for the hyperfine-induced geminate recombination process.

In the case of large DMA concentration, the bimolecular electron exchange reaction[15]

$$^2DMA^+ + {}^1DMA \rightarrow {}^1DMA + {}^2DMA^+$$

may become fast compared to the hyperfine induced spin motion. The magnetic moments of the nuclei on the DMA^+ radicals "seen" by the unpaired electron spin are expected then to average to zero, and only the hyperfine coupling in the pyrene radical anion determines the singlet–triplet transition probability of the pair $^2Py^- + {}^2e^+$ ($^2e^+$ indicates a doublet electron "hole" hopping between donor molecules in the solution). The time evolution of the triplet probability for this system is presented in Fig. 2 for various field strengths. In these calculations we have again employed the hyperfine coupling constants (3.9). Due to the smaller hyperfine interaction in this case the initial rise of the triplet probability is much slower than in Fig. 1. It is interesting to note that the triplet probability curve for $B = 0$ is below the $B \to \infty$ curve at times larger than 25 ns. However, already in the presence of very weak magnetic fields ($B = 5$ G) the oscillation seen in the $B = 0$ curve is dampened, and there is a considerable increase of the triplet probability with respect to the $B = 0$ curve at times $t > 15$ ns.

A lowering of the hyperfine-induced singlet – triplet transition probability is predicted if the protons are substituted by deuterons. This effect is due to the smaller magnetogyric ratio of the deuteron with respect to the proton[16] which results in a lowering of the hyperfine coupling constants by a factor of 6.514. This effect is partly compensated by the increase of the nuclear spin from $\frac{1}{2}$ to 1. The time evolution of the triplet probability for perdeuterated pyrene (^2d-$Py^- + {}^2e^+$) is indicated by the dashed and dash–dotted curves in Fig. 2 for $B = 0$ and $B \to \infty$, respectively. The initial rise of the triplet probability of the perdeuterated system is observed to be slower by a factor of about 4.

The number of nuclear spin states is much larger in perdeuterated radicals (3^N instead of 2^N for N nuclei). Therefore we could not evaluate the triplet probability of the system ^2d-$Py^- + {}^2d$-DMA^+ at low field strengths. For high fields, however, the analytical expression of Brocklehurst[9] can be applied. In Fig. 3 the triplet probabilities $p_T^0(t)$ for the systems $^2Py^- + {}^2DMA^+$ and ^2d-$Py^- + {}^2d$-DMA^+ (all protons substituted by deuterons) are compared. In this case, the isotope effect is much less pronounced than in Fig. 2. This is due to the large hyperfine coupling constant of the nitrogen atom on $^2DMA^+$ which remains unaltered upon deuteration. The predominant coupling of the N atom also brings about the oscillations of the triplet probability of the perdeuterated pair. At zero magnetic field the oscillatory behavior should be even more pronounced, as has been discussed recently by Brocklehurst.[9]

IV. FINITE-DIFFERENCE APPROXIMATION FOR THE SOLUTION OF THE LIOUVILLE EQUATION–TEST OF THE APPROXIMATE LIOUVILLE EQUATION (2.19)

As discussed in Sec. II for the case $\kappa_S = \kappa_T$, the stochastic Liouville equation for the geminate processes of an isolated radical pair (2.10) can be separated into the diffusion equation (2.12) and a Liouville equation for the spin motion of the radicals (2.13). In order to integrate the diffusion equation (2.12) a finite-difference method has been introduced[11,17] which assumes a discretization r_α, $\alpha = 1, 2, \ldots, N$ of the radial coordinate r. The continuous pair distribution function $d(r, t)$ is then represented by a vector $\mathbf{d}(t)$ with components

$$d^\alpha(t) = d(r_\alpha, t) \tag{4.1}$$

and the diffusion operator $l(r)$ [Eq. (2.3)] is replaced by a tridiagonal matrix L with elements[11] ($2 \leq \alpha \leq N-1$, $h_\alpha = r_{\alpha+1} - r_\alpha$)

$$L^{\alpha\alpha} = -D\left(\frac{2}{h_\alpha h_{\alpha-1}} + \beta\frac{r_{\alpha+1}^2 F(r_{\alpha+1}) - r_{\alpha-1}^2 F(r_{\alpha-1})}{r_\alpha^2(h_\alpha + h_{\alpha-1})}\right), \tag{4.2a}$$

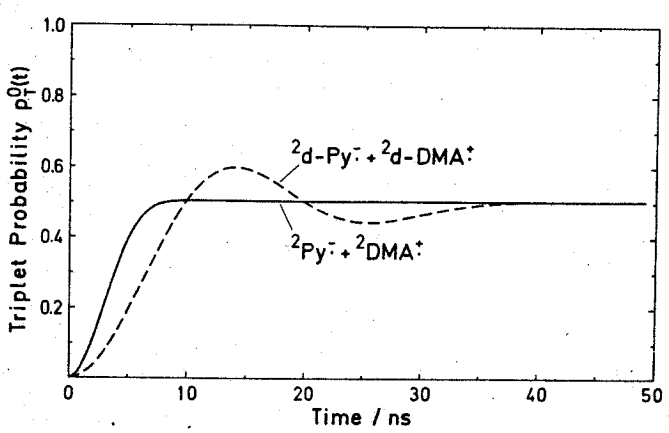

FIG. 3. Time evolution of the triplet probability $p_T^0(t)$ for the systems $^2Py^- + {}^2DMA^+$ and ^2d-$Py^- + {}^2d$-DMA^+ (all protons substituted by deuterons) for high magnetic fields ($B \to \infty$).

$$L^{\alpha\alpha+1} = D\left(\frac{r_{\alpha+1}}{r_\alpha}\frac{2}{h_\alpha(h_\alpha+h_{\alpha-1})} - \beta\frac{F(r_\alpha)}{h_\alpha+h_{\alpha-1}}\right), \quad (4.2b)$$

$$L^{\alpha\alpha-1} = D\left(\frac{r_{\alpha-1}}{r_\alpha}\frac{2}{h_{\alpha-1}(h_\alpha+h_{\alpha-1})} + \beta\frac{F(r_\alpha)}{h_\alpha+h_{\alpha-1}}\right), \quad (4.2c)$$

$$L^{11} = -\frac{V_2}{V_1}L^{21}, \quad (4.2d)$$

$$L^{12} = -\frac{V_2}{V_1}L^{22} - \frac{V_3}{V_1}L^{32}, \quad (4.2e)$$

$$L^{NN} = -\frac{V_{N-1}}{V_N}L^{N-1N}, \quad (4.2f)$$

$$L^{N-1N} = -\frac{V_{N-1}}{V_N}L^{N-1N-1} - \frac{V_{N-2}}{V_N}L^{N-2N-1}, \quad (4.2g)$$

where V_i are the discrete volume elements:

$$V_\alpha = \begin{cases} 2\pi r_\alpha^2(h_\alpha+h_{\alpha-1}) & 2\leq\alpha\leq N-1 \\ 2\pi r_1^2 h_1 & \alpha=1 \\ 2\pi r_N^2 h_{N-1} & \alpha=N. \end{cases}$$

$F(r_\alpha)$ is the force acting between the radicals at distance r_α, e.g., a Coulomb force $F(r_\alpha) = -e^2/\epsilon r_\alpha^2$. The diffusion equation is then approximated by the differential–difference equation

$$\dot{\mathbf{d}}(t) = (\mathbf{L}-\mathbf{U})\,\mathbf{d}(t), \quad (4.3)$$

where the diagonal matrix $\mathbf{U}$ accounts for the radical recombination

$$U^{\alpha\alpha} = \kappa s(r_\alpha). \quad (4.4)$$

The matrix elements (4.2d)–(4.2g) follow from the particle conservation requirement in the case $\kappa = 0$,[11,17] i.e.,

$$\sum_j\left(\sum_i V_i L^{ij}\right)d_j = 0.$$

Since this equation must hold for any arbitrary distribution $\mathbf{d}$, each term must vanish:

$$\sum_i V_i L^{ij} = 0.$$

This is fulfilled for the matrix $\mathbf{L}$ as defined above.

The formal solution of (4.3) is

$$\mathbf{d}(t) = \exp[(\mathbf{L}-\mathbf{U})t]\,\mathbf{d}(0), \quad (4.5)$$

which had been evaluated in Ref. 11 by an eigenvector expansion (*Method* 1).

Here, we will integrate (4.3) by also discretizing the time t (t_β, $\beta = 1,2,\ldots$) employing the Crank–Nicholson implicit integration scheme[18a] ($\Delta t_\beta = t_{\beta+1} - t_\beta$)

$$\mathbf{d}(t_{\beta+1}) = \mathbf{d}(t_\beta) + \tfrac{1}{2}\Delta t_\beta(\mathbf{L}-\mathbf{U})[\mathbf{d}(t_\beta)+\mathbf{d}(t_{\beta+1})], \quad (4.6)$$

and solving for $\mathbf{d}(t_{\beta+1})$. As $(\mathbf{L}-\mathbf{U})$ is a tridiagonal matrix, Eq. (4.6) can be solved efficiently by means of a recursion method.[18b] We will refer to this solution of the diffusion equation as *Method* 2. Once the pair distribution function has been determined, the geminate recombination yields can be evaluated according to Eqs. (2.14) and (2.20) through

$$\phi^{\rm gem}_{S\to S,T}(t) = \int_0^t d\tau\, p^0_{S,T}(\tau)\sum_{\alpha=1}^N V_\alpha U^{\alpha\alpha}\; d^\alpha(\tau) \quad (4.7a)$$

or, employing the trapezoidal rule for the time integration,

$$\phi_{S\to S,T}(t_{\beta+1}) = \phi^{\rm gem}_{S\to S,T}(t_\beta) + (\Delta t_\beta/2)\sum_{\alpha=1}^N V_\alpha U^{\alpha\alpha} \times[p^0_{S,T}(t_\beta)d^\alpha(t_\beta) + p^0_{S,T}(t_{\beta+1})d^\alpha(t_{\beta+1})]. \quad (4.7b)$$

The finite-difference Method 2 has the important advantage over Method 1 that it can also be employed in the general case $\kappa_S \neq \kappa_T$ for the solution of the exact Liouville equation (2.10) [or (2.15)] and its approximate version (2.19). In order to integrate Eq. (2.19) the continuous distributions $p_S(r,t)$ and $p_T(r,t)$ are represented by distribution vectors $\mathbf{p}_S(t_\beta)$ and $\mathbf{p}_T(t_\beta)$ with the components $p^\alpha_S(t_\beta) = p_S(r_\alpha, t_\beta)$ and $p^\alpha_T(t_\beta) = p_T(r_\alpha, t_\beta)$, respectively. The integration of Eq. (2.19) is then carried out by means of

$$\mathbf{p}_S(t_{\beta+1}) = \mathbf{p}_S(t_\beta) + \tfrac{1}{2}\Delta t_\beta(\mathbf{L}-\mathbf{U}_S)[\mathbf{p}_S(t_\beta)+\mathbf{p}_S(t_{\beta+1})] + \Delta t_\beta \dot{p}^0_S[\tfrac{1}{2}(t_\beta+t_{\beta+1})][\mathbf{p}_S(t_\beta)+\mathbf{p}_T(t_\beta)], \quad (4.8a)$$

$$\mathbf{p}_T(t_{\beta+1}) = \mathbf{p}_T(t_\beta) + \tfrac{1}{2}\Delta t_\beta(\mathbf{L}-\mathbf{U}_T)[\mathbf{p}_T(t_\beta)+\mathbf{p}_T(t_{\beta+1})] + \Delta t_\beta \dot{p}^0_T[\tfrac{1}{2}(t_\beta+t_{\beta+1})][\mathbf{p}_S(t_\beta)+\mathbf{p}_T(t_\beta)], \quad (4.8b)$$

where the diagonal matrices $\mathbf{U}_S$ and $\mathbf{U}_T$ are defined through

$$U^{\alpha\alpha}_S = s(r_\alpha)\kappa_S \text{ and } U^{\alpha\alpha}_T = s(r_\alpha)\kappa_T. \quad (4.9)$$

We will refer to the solution of the approximate Liouville equation (2.19) by means of (4.8) as *Method* 3. In this integration scheme the coupling terms $\dot{p}^0_{S,T}[\frac{1}{2}(t_\beta + t_{\beta+1})][\mathbf{p}_S(t_\beta)+\mathbf{p}_T(t_\beta)]$ accounting for the singlet–triplet spin transitions are treated explicitly, i.e., $\mathbf{p}_S(t)+p_T(t)$ is taken only at the past time t_β and not at $t_{\beta+1}$. The coupling terms are then trivially included in the same recursive algorithm as employed before for the integration of Eq. (4.3). The explicit integration of the coupling terms makes it necessary, however, to choose the time steps Δt_β smaller than in the case of Eq. (4.6), in particular at short times for which $\mathbf{p}_S + \mathbf{p}_T$ is varying rapidly. In the course of evaluating the distributions $\mathbf{p}_{S,T}(t_{\beta+1})$ the singlet and triplet geminate recombination yields are obtained through

$$\phi^{\rm gem}_{S\to S,T}(t_{\beta+1}) = \phi^{\rm gem}_{S\to S,T}(t_\beta) + (\Delta t_\beta/2)\sum_\alpha V_\alpha U^{\alpha\alpha} \times[p^\alpha_{S,T}(t_\beta) + p^\alpha_{S,T}(t_{\beta+1})]. \quad (4.10)$$

For the integration of the exact Liouville equation (2.15) we will apply the Crank–Nicholson scheme in a somewhat modified form. Representing the real and imaginary parts of the density matrix $R_{ij}(r,t)$ and $S_{ij}(r,t)$, respectively, by the distribution vectors $\mathbf{R}_{ij}(t_\beta)$ and $\mathbf{S}_{ij}(t_\beta)$ with the components

$$R^\alpha_{ij}(t_\beta) = R_{ij}(r_\alpha, t_\beta), \quad (4.11a)$$

$$S^\alpha_{ij}(t_\beta) = S_{ij}(r_\alpha, t_\beta), \quad (4.11b)$$

the integration of (2.15) proceeds through the scheme

$$\mathbf{S}_{ij}(\tau_{\beta+1}) = \mathbf{S}_{ij}(\tau_\beta) + \tfrac{1}{2}\Delta\tau_\beta[\mathbf{L}-\mathbf{U}_{ii}-\mathbf{U}_{jj}][\mathbf{S}_{ij}(\tau_\beta)+\mathbf{S}_{ij}(\tau_{\beta+1})] + \Delta\tau_\beta\mathbf{E}_{ij}[\mathbf{R}(t_\beta)], \quad (4.12a)$$

TABLE I. Test of computational methods—geminate recombination of freely diffusing radicals ($\kappa_S = \kappa_T$).[a]

Time (ns)	Exact	Method 1	Method 2	Method 3	Method 4
			$\phi^{gem}_{S\to S}(t)$		
10	0.2002[b]	0.2002[c]	0.2002[d]	0.2001[d]	0.2002[d]
20	0.2032	0.2032	0.2032	0.2031	0.2032
30	0.2051	0.2051	0.2051	0.2051	0.2051
40	0.2059	0.2059	0.2059	0.2060	0.2059
50	0.2066	0.2066	0.2066	0.2066	0.2066
			$\phi^{gem}_{S\to T}(t)$		
10	0.02674[b]	0.02674[c]	0.02674[d]	0.02681[d]	0.02672[d]
20	0.03031	0.03031	0.03031	0.03040	0.03029
30	0.03144	0.03145	0.03146	0.03142	0.03141
40	0.03240	0.03241	0.03241	0.03235	0.03238
50	0.03295	0.03295	0.03296	0.03297	0.03293

[a] $D = 10^{-5}$ cm^2 s^{-1}, $\kappa_S = \kappa_T = 4.762$ Å ns^{-1}, which corresponds to a value of 0.25 for the total recombination yield, one proton on each radical with $a_1 = a_2 = 50$ G at a magnetic field $B = 0$ G.

[b] Analytical expression from Ref. 11.

[c] As defined in the text with the spatial discretization (in units of Å) $h = 0.5$ ($7 \le r \le 20$), $h = 1.0$ ($20 < r \le 50$), $h = 2.0$ ($50 < r \le 100$), $h = 20.0$ ($100 < r \le 500$).

[d] As defined in the text with a space discretization as for Method 1 and the time discretization (Δt in units h_1^2/D) $\Delta t = 0.5$ ($0 \le t \le 0.01$ ns), $\Delta t = 1.0$ (0.01 ns $< t \le 0.1$ ns), $\Delta t = 5.0$ (0.1 ns $< t \le 5$ ns), $\Delta t = 10.0$ (5 ns $< t \le 50$ ns).

$$\mathbf{R}_{ij}(t_{\beta+1}) = \mathbf{R}_{ij}(t_\beta) + \tfrac{1}{2}\Delta t_\beta [\mathbf{L} - \mathbf{U}_{ii} - \mathbf{U}_{jj}][\mathbf{R}_{ij}(t_\beta) + \mathbf{R}_{ij}(t_{\beta+1})] + \Delta t_\beta \mathbf{D}_{ij}[\mathbf{S}(\tau_{\beta+1})] , \quad (4.12b)$$

where the vectors $\mathbf{D}_{ij}[\mathbf{R}(t)]$ and $\mathbf{E}_{ij}[\mathbf{S}(t)]$ have the components

$$D^\alpha_{ij}[\mathbf{S}(t)] = \frac{1}{\hbar} \sum_{k\neq i,\,j} [H_{ik} S^\alpha_{kj}(t) + H_{jk} S^\alpha_{ki}(t)] + \frac{1}{\hbar}[H_{ii}(r_\alpha) - H_{jj}(r_\alpha)] S^\alpha_{ij}(t) , \quad (4.13a)$$

$$E^\alpha_{ij}[\mathbf{R}(t)] = -\frac{1}{\hbar}\left(\sum_{k\neq i} H_{ik} R^\alpha_{kj}(t) - \sum_{k\neq j} H_{jk} R^\alpha_{ki}(t)\right) - \frac{1}{\hbar}[H_{ii}(r_\alpha) - H_{jj}(r_\alpha)] R^\alpha_{ij}(t) . \quad (4.13b)$$

The diagonal matrix $\mathbf{U}$ is defined through

$$U^{\alpha\alpha}_{ii} = \tfrac{1}{2} s(r_\alpha)(\kappa_S Q^{ii}_S + \kappa_T Q^{ii}_T) , \quad (4.13c)$$

and $\Delta t_\beta = t_{\beta+1} - t_\beta$; $\Delta\tau_\beta = \tau_{\beta+1} - \tau_\beta$; $\tau_\beta = (t_\beta + t_{\beta-1})/2$.

We will refer to the solution of the exact Liouville equation by means of these equations as *Method* 4. In this integration scheme one computes at each time step first the vectors $\mathbf{S}_{ij}(\tau_{\beta+1})$ employing in the coupling term $\mathbf{E}_{ij}[\mathbf{R}(t_\beta)]$ the vectors $\mathbf{R}_{ij}(t_\beta)$, and in the second step computes the vectors $\mathbf{R}_{ij}(t_{\beta+1})$, employing the newly evaluated $\mathbf{S}_{ij}(\tau_{\beta+1})$ in the coupling term $\mathbf{D}_{ij}[\mathbf{S}(\tau_{\beta+1})]$. This way of interweaving the integration of $\mathbf{R}_{ij}$ and $\mathbf{S}_{ij}$ greatly improves the accuracy of the explicit integration of the coupling terms and, hence, one can choose rather large time steps Δt_β as in the case of Eq. (4.6).

The geminate recombination yields $\phi^{gem}_{S\to S,T}$ are evaluated according to

$$\phi^{gem}_{S\to S,T}(t_{\beta+1}) = \phi^{gem}_{S\to S,T}(t_\beta) + \Delta t_\beta \sum_\alpha V_\alpha \mathrm{Tr}\{\mathbf{Q}_{S,T} U^{\alpha\alpha}[\mathbf{R}^\alpha(t_\beta) + \mathbf{R}^\alpha(t_{\beta+1})]\} , \quad (4.14)$$

where V_α has been defined above.

In Eq. (4.12), each n-dimensional block of the spin Hamiltonian H couples $n(n+1)/2$ elements R^α_{ij} and $n(n-1)/2$ elements S^α_{ij} for each distance r_α. The diffusion operator $\mathbf{L}$ in turn couples all N submatrices R^α and S^α; hence, Eq. (4.12) comprises Nn^2 coupled equations. At low fields the block dimensions n increase rapidly with the number of nuclear spins and Method 4 can be applied only to very simple radical pair systems. For a radical pair with one proton on each molecule with identical hyperfine coupling constants and $g_1 = g_2$, the density matrix reduces to four nonzero blocks, one of dimension 4 and three of dimension 2. Thus, even for this simple model, 28 diffusion equations have to be integrated. Choosing a rather coarse spatial discretization scheme with $N = 50$, Eq. (4.12) comprises for the largest block of the density matrix a set of 800 (!) coupled equations. Therefore, large nuclear spin systems on the radical pairs cannot be treated within the framework of the exact Liouville equation (2.10) (except for high magnetic field strengths) and the approximate Liouville equation (2.19) must be employed. However, this is no problem, as we will demonstrate below that (2.19) provides an excellent approximation to the exact Liouville equation.

For high magnetic fields ($B \to \infty$) the $T_{\pm 1}$ electron spin states are decoupled from the S, T_0 states and the Hamiltonian decomposes into 2×2 blocks coupling the $|S,N\rangle$ and the $|T_0,N\rangle$ states for each nuclear spin configuration N. If the exchange interaction $J(r)$ is neglected, the Liouville equation (2.15) gives rise to only three coupled diffusion equations for each nonequivalent block of the Hamiltonian. In this case the exact Liouville equation (2.15) can be solved numerically also for radical pair systems with a large number of nuclear spins.

We want to demonstrate now the numerical accuracy of the finite-difference integration schemes (Methods 1–4) presented above. Let us first consider the case $\kappa_S = \kappa_T$. Since in this case the Liouville equation (2.19) holds rigorously, all four methods are expected to yield exact results. For radicals undergoing *free Brownian motion* with a recombination domain defined through $s(r) = \delta(r - r_1)$, an analytical expression for the singlet and triplet recombination yields had been derived in Ref. 11. This provides a direct check of the numerical results of Methods 1–4. In Table I the geminate recombination yields of all four computational methods are compared with the analytical values at times 10 ns, 20 ns, ..., 50 ns, for a radical pair system with the hyperfine coupling constants $a_1 = a_2 = 50$ G, at $B = 0$ G, in a solvent medium with $D = 10^{-5}$ cm^2 s^{-1}, and $\kappa_S = \kappa_T = \kappa = 4.762$ Å ns^{-1} corresponding to a total recombination yield of 25%. The errors in the yields are found to be all less than 0.1%, demonstrating that the discretization of the diffusion space in Method 1 and the additional discretization of time in Methods 2, 3, and 4, as specified below

TABLE II. Test of computational methods —geminate recombination of radical ion pairs ($\kappa_S = \kappa_T$).[a]

Time (ns)	Method 1[b]	Method 2[b]	Method 3[b]	Method 4[b]
		$\phi^{gem}_{S\to S}(t)$		
10	0.5886	0.5883	0.5880	0.5884
20	0.6016	0.6013	0.6009	0.6014
30	0.6087	0.6084	0.6085	0.6086
40	0.6118	0.6116	0.6117	0.6117
50	0.6143	0.6140	0.6141	0.6142
		$\phi^{gem}_{S\to T}(t)$		
10	0.1438	0.1437	0.1441	0.1436
20	0.1589	0.1589	0.1593	0.1588
30	0.1634	0.1633	0.1633	0.1631
40	0.1669	0.1669	0.1668	0.1667
50	0.1689	0.1689	0.1689	0.1687

[a] $D = 10^{-5}$ cm^2 s^{-1}, $\kappa_S = \kappa_T = 4.762$ Å/ns, which corresponds to a value of 0.6264 for the total yield of geminate recombination, solvent polarity $\epsilon = 20$, $T = 25$ °C, one proton on each radical with $a_1 = a_2 = 50$ G at a magnetic field $B = 0$ G.

[b] As defined in the text with the space and time discretization in Table I.

Table I, ensure an accurate description of the geminate recombination process.

Table II exhibits the geminate recombination yields for *radical ions* in a polar solvent with $\epsilon = 20$ as evaluated by Methods 1, 2, 3, and 4 (at $T = 25$ °C, the other parameters as for Table I). The results of the four methods again differ by only 0.1%, proving that no significant numerical errors arise in the presence of a Coulomb force field acting between the radical ions.

In our calculations we found Method 2, which entails both time and space discretization, to be more efficient than Method 1, in which the time integration is performed by an eigenvector expansion. For the examples presented in Tables I and II, a computation time of 15 s on an Univac 1108 installation was needed for the evaluation of the yields $\phi^{gem}_{S\to S,T}$ (50 ns) by means of Method 2, whereas the matrix diagonalization to obtain the eigenvalues and eigenvectors alone in Method 1 required 35 s. Because of the core space requirements of the eigenvalue problem, the allowable dimension N of the matrix L, and consequently the size of the integration domain and space partitions, are much more limited in Method 1.

In the case $\kappa_S \neq \kappa_T$, the Liouville equation (2.10) needs to be solved by Method 4 and its approximate version (2.19) by Method 3. In the following we will demonstrate the validity of Eq. (2.19) by comparing its predictions with the results of the exact Liouville equation. For low fields this demonstration has to be restricted to the simple two proton radical pair system already considered above (Tables I, II) as the exact Liouville equation cannot be solved for larger spin systems. The singlet and triplet geminate recombination yields $\phi^{gem}_{S\to S}(t)$ and $\phi^{gem}_{S\to T}(t)$, respectively, resulting from the exact and the approximate Liouville equation, are presented in Fig. 4(a) for a radical ion pair system with hyperfine coupling constants $a_1 = a_2 = 20$ G, at $B = 0$ G, in a solvent medium with $D = 10^{-5}$ cm^2 s^{-1}, $\epsilon = 30$ at $T = 25$ °C, and $\kappa_S = 0.9468$ Å ns^{-1} and $\kappa_T = 2.8403$ Å ns^{-1} corresponding to recombination probabilities of 25% and 50%, respectively.[19] In order to reduce the computation time we have chosen a discretization of the radial coordinate coarser than the one in Table I. The singlet yield $\phi^{gem}_{S\to S}(t)$ exhibits initially a sharp rise and levels off to a value 16.8% at 50 ns, whereas the triplet yield $\phi^{gem}_{S\to T}(t)$ is found to increase more slowly and reaches its saturation value only at longer times (11.2% at 50 ns). Up to about 10 ns, the exact and the approximate yield curves are very close. An error builds up, however, in the time interval between 10 and 20 ns and stays nearly constant from thereon. Fifty nanoseconds after pair generation the absolute error in the triplet yield is -0.3% and on the singlet yield is $+0.1$%. This demonstrates that the suppression of the singlet↔triplet transition probability in the reaction domain, as discussed in Ref. 2, is overcompensated by an increase of the transition probability outside the reaction domain

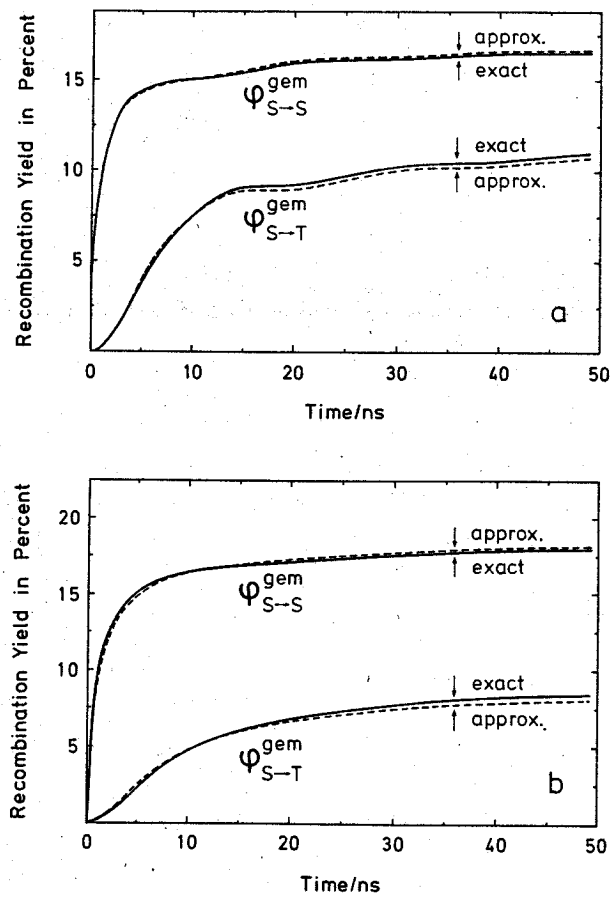

FIG. 4. Time evolution of the singlet and triplet geminate recombination yields resulting from the exact Liouville equation (2.10) as evaluated according to Eq. (4.12) (Method 4) and from the approximate Liouville equation (2.19) as evaluated according to Eq. (4.8) (Method 3). The space discretization is given below Table III. For the time discretization see below Table I (exact yields) and below Table III (approximate yields). (a) Radical ion pair system with one proton spin on each radical at zero magnetic field ($D = 10^{-5}$ cm^2 s^{-1}, $\epsilon = 30$, $T = 25$ °C, $\kappa_s = 0.9468$ Å/ns, $\kappa_T = 2.8403$ Å/ns, $a_1 = a_2 = 20$ G; (b) $^2Py^- + {}^2DMA^+$ radical pair system at high magnetic field ($B \to \infty$) [$D = 10^{-5}$ cm^2 s^{-1}, $\epsilon = 30$, $T = 25$ °C, $\kappa_S = 0.9468$ Å/ns, $\kappa_T = 2.8403$ Å/ns, hyperfine coupling constants (3.9) and (3.10)].

TABLE III. Effect of the exchange interaction on the geminate recombination of a model radical ion pair system[a] in a solvent $\epsilon = 30$.

Model[b]	$\phi_S(B=0)$[c]	$\phi_S(B=200)$	$\phi_T(B=0)$[c]	$\phi_T(B=200)$	$\frac{\phi_T(B=200)}{\phi_T(B=0)}$
I	0.161	0.182	0.093	0.048	0.512
II	0.165	0.183	0.085	0.045	0.532
III	0.169	0.185	0.076	0.041	0.546

[a] One proton on each radical with $a_1 = a_2 = 20$ G, $D = 10^{-5}$ cm^2 s^{-1}, $T = 25$ °C, $\kappa_S = 0.9468$ Å/ns (i.e., total yield of 25% for $\epsilon = 30$), $\kappa_T = 2.84$ Å/ns (i.e., total yield of 50% for $\epsilon = 30$).[19] Spatial discretization (in units of Å) employed in the finite difference method: $h = 1$ ($7 \le r \le 20$), $h = 2$ ($20 < r \le 40$), $h = 3$ ($40 < r \le 100$), $h = 20$ ($100 < r \le 200$). Time discretization (Δt in units h_1^2/D): $\Delta t = 0.1$ ($0 \le t \le 0.01$ ns), $\Delta t = 1.0$ (0.01 ns $< t \le 5$ ns), $\Delta t = 2.5$ ($t > 5$ ns).

[b] I: no exchange interaction; II: $J(r) = 200$ G (7 Å $\le r \le 7.5$ Å), $J(r) = 0$ G ($r > 7.5$ Å); III: $J(r) = 100$ G (7 Å $\le r \le 7.5$ Å), $J(r) = 75$ G (7.5 Å $< r \le 8.5$ Å), $J(r) = 50$ G (8.5 Å $< r \le 9.5$ Å), $J(r) = 25$ G (9.5 Å $< r \le 10.5$ Å), $J(r) = 0$ ($r > 10.5$ Å).

[c] Yields are taken at 50 ns after pair generation, $\phi_{S,T}(B) = \phi^{gem}_{S\to S,T}(50\text{ ns}, B)$, B in units of gauss.

due to a predominant loss of the triplet components of the spin wavefunction (for $\kappa_T > \kappa_S$). As to be expected, the error in the geminate recombination yields is found to be somewhat larger for the radical ion recombination in a less polar medium with $\epsilon = 20$ (the other parameters as before):

$\phi^{gem}_{S\to T}$(50 ns): 15.3% (exact), 14.7% (approx.),

$\phi^{gem}_{S\to S}$(50 ns): 13.8% (exact), 14.1% (approx.).

[same discretization as for Fig. 4(a)].

For higher magnetic fields the approximate Liouville equation (2.19) can also be tested for radical pairs with large nuclear spin systems. We have carried out this test for the system ^{2}Py$^-$ + ^{2}DMA$^+$ with the hyperfine coupling situation described by (3.9) and (3.10). In Fig. 4(b) the exact results based on Eq. (2.15) are found in excellent agreement with the approximate results based on Eq. (2.19). We may point out that the exact solution of (2.15) requires the integration of 675 diffusion equations, whereas the approximate version (2.19) requires only the integration of two coupled diffusion equations. The error in the approximate description (2.19) mainly arises through the averaging over all nuclear spin states which introduces the transition rate $\dot{p}^0_S(t)$ as the driving term connecting singlet and triplet radical pair states. At longer times $\dot{p}^0_S(t)$ vanishes, although the transition rate contributions of each nuclear spin state does not vanish and in the exact description continues to transfer radical pairs from the singlet to the triplet electron spin state and *vice versa*. The close agreement between the approximate and the exact results encouraged us to base in Sec. VII our investigations of the solvent and temperature dependence of the geminate recombination of the pyrene–DMA radical pair on the approximate Liouville equation (2.19).

V. THE EFFECT OF AN EXCHANGE INTERACTION $J(r)$ IN THE CONTACT REGION OF A RADICAL PAIR

For an account of the effect of an exchange interaction $J(r)$ on the geminate recombination of radical pairs, we consider again the two-proton radical pair system of Sec. IV, since only for this simple model system can the exact Liouville equation (2.10) be solved numerically. The exchange interaction lifts the degeneracy between the singlet and triplet electron spin states and, hence, reduces the singlet↔triplet transition probability in the contact region. As the strength of the hyperfine interaction amounts only to about 10^{-6} eV, very weak exchange interactions suffice to influence the geminate recombination. Unfortunately, nothing is known about the magnitude of $J(r)$ or the domain over which it is acting. As $J(r)$ is approximately proportional to the overlap of the orbitals of the unpaired electrons in the two radicals, it is expected to decrease rapidly with increasing radical separation.

In Tables III and IV we have compared three different models for the exchange interaction: (1) $J(r) = 0$; (2) $J(r) = 200$ G in the first space interval and zero elsewhere, such that the hyperfine induced spin motion is completely prevented in the contact region; (3) $J(r)$ is a decreasing step function extending over a distance of 3.5 Å (see below Table III).

In all cases the recombination is assumed to take place only in the first space interval (7 Å, 7.5 Å). The calculations are based on the two-proton radical pair system of Tables III and IV with hyperfine coupling constants $a_1 = a_2 = 20$ G, in solvents with $D = 10^{-5}$ cm^2 s^{-1} and $\epsilon = 30$ and $\epsilon = 20$, respectively. The rate constants κ_S and κ_T correspond to 25% and 50% recombination probability.[19] We have evaluated the recombination yields only up to 20 ns, at which time the yields have achieved 80%–90% of their final values. Tables III and IV demonstrate that the effect of the exchange interaction on the singlet yield $\phi^{gem}_{S\to S}$(20 ns, $B = 0$) is negligible. However, for the radical pair models (1), (2), and (3) in a solvent with $\epsilon = 30$, the triplet yield $\phi^{gem}_{S\to T}$(20 ns, $B = 0$) decreases from 9.3% to 8.5% and 7.6%, respectively, reflecting the suppression of the singlet↔triplet transitions through $J(r)$. As is to be expected, this effect is more pronounced in a less polar solvent with $\epsilon = 20$ (12.3%, 9.5%, 8.3%) as the stronger Coulomb attraction keeps more pairs in the contact region. The influence of the exchange interaction is stronger at low magnetic field strengths than at high fields, and hence, the magnetic field effect $\phi^{gem}_{S\to T}$(20 ns, $B = 200$ G)/$\phi^{gem}_{S\to T}$(20 ns, $B = 0$) increases slightly as demonstrated in Tables III and IV.

From the above results it is apparent that the effect of the exchange interaction on the radical ion recombi-

TABLE IV. Effect of the exchange interaction on the geminate recombination of a model radical ion pair system[a] in a solvent $\epsilon = 20$.

Model[b]	$\phi_S(B=0)$[c]	$\phi_S(B=200)$	$\phi_T(B=0)$[c]	$\phi_T(B=200)$	$\frac{\phi_T(B=200)}{\phi_T(B=0)}$
I	0.128	0.154	0.123	0.064	0.518
II	0.141	0.160	0.095	0.052	0.546
III	0.147	0.163	0.083	0.046	0.561

[a] See Table III.

[b] See Table III.

[c] $\phi_{S,T}(B) = \phi^{gem}_{S\to S,T}$ (20 ns, B), B in units of gauss.

TABLE V. Relative diffusion coefficients[a] $D = D^{25}_{Py} + D^{25}_{DMA}$ and dielectric constants[b] for various solvents at $T = 25\,^{\circ}C$.

Solvent	$D \times 10^5$ ($cm^2\ s^{-1}$)	ϵ
ACN[c]	4.53	37.5
CH_3OH	2.85	32.6
DMF[d]	1.96	37.6
C_2H_5OH	1.44	25.2
C_3H_7OH	0.77	19.7

[a]Reference 21. [c]Acetonitrile.
[b]Reference 22. [d]*N*,*N*-dimethylformamide.

nation, i.e., a reduction of the triplet yield $\phi^{gem}_{S\to T}$ and a slight increase of the singlet yield $\phi^{gem}_{S\to S}$, depends on the polarity of the solvent. In polar solvents, such as acetonitrile, dimethylformamide, or methanol, the effect of the exchange interaction can be neglected to a good approximation.

VI. THE RELATIONSHIP BETWEEN THE GEMINATE RECOMBINATION RATE CONSTANTS κ_S, κ_T AND THE SECOND-ORDER HOMOGENEOUS RATE CONSTANTS

The geminate recombination yields are functions of the recombination rate constants κ_S and κ_T in the Liouville equation (2.1). In this section we will provide the relationship between these quantities and second-order recombination rate constants which are amenable to experimental determination.[5,6] The following discussion holds, however, only for low concentrations of the radicals, i.e., assumes that the average time between diffusion-controlled radical encounters is much longer than the time course of the geminate recombination process.

In the case of equal singlet and triplet recombination rate constants κ_S and κ_T, respectively, the overall homogeneous recombination rate constant k_{rec} is given by

$$k_{rec} = \phi k_d \ , \tag{6.1}$$

where ϕ represents the total yield of geminate recombination and k_d the diffusion-controlled homogeneous recombination rate constant. ϕ and k_d are given by the expressions[20] ($\kappa_S = \kappa_T = \kappa$)

$$k_d = 4\pi N_L D r_L/(1 - e^{-r_L/r_1}) \ , \tag{6.2}$$

$$\phi = 1/(1 + k_b/\kappa') \ , \tag{6.3}$$

where r_L is the Onsager radius, $r_L = e^2/\epsilon kT$, and N_L is Avogadro's number. $\kappa' = \kappa/\Delta r$ presents the first-order recombination rate constant in the reaction domain with width Δr.

k_b represents the rate constant of separation for the encounter complex ($^2A^{\cdot-} + {}^2D^{\cdot+}$),

$$k_b = \frac{D}{\Delta r\, r_1^2} \frac{r_L}{e^{r_L/r_1} - 1} \ . \tag{6.4}$$

In Eqs. (6.2)–(6.4) it is assumed that the radicals recombine at the distance r_1, i.e., $s(r) = \delta(r - r_1)$. The microscopic rate constant κ can then be determined from the measured bimolecular rate constant k_{rec}.

Unfortunately, such a simple relationship does not exist if $\kappa_S \neq \kappa_T$. In this case the total (singlet + triplet) yield of geminate recombination depends on the spin motion of the radical pair. At low concentrations the total bimolecular rate constant is given by

$$k_{rec} = k_d\,[0.25(\phi^{gem}_{S\to S} + \phi^{gem}_{S\to T}) + 0.75(\phi^{gem}_{T\to S} + \phi^{gem}_{T\to T})] \ . \tag{6.5}$$

This formula implies that 25% of the random encounters occur initially in the singlet electron spin state giving rise to a total recombination yield $\phi^{gem}_{S\to S} + \phi^{gem}_{S\to T}$, and 75% occur initially in a triplet state with a total recombination yield $\phi^{gem}_{T\to S} + \phi^{gem}_{T\to T}$. These yields depend implicitly on κ_S and κ_T. To determine these two rate constants a second experimental parameter is needed. The most appropriate choice is the homogeneous triplet recombination rate constant k^T_{rec} which is related to the yields of geminate triplet products $\phi^{gem}_{S\to T}$ and $\phi^{gem}_{T\to T}$ through the expression

$$k^T_{rec} = k_d\,(0.25\phi^{gem}_{S\to T} + 0.75\phi^{gem}_{T\to T}) \ . \tag{6.6}$$

As an example we have estimated the rate constants κ_S and κ_T for the system Py–DMA in acetonitrile. Since the bimolecular rate constants k_{rec} and k^T_{rec} have not been determined yet for this system, we have assumed that they are identical to those of the closely related system pyrene–*N*,*N*-diethylaniline (Py–DEA)[5]: $k_{rec} = (4.2 \pm 0.3)10^{10}$ $dm^3\ mole^{-1}$ and $k^T_{rec} = (4.0 \pm 0.3)\ 10^{10}$ $dm^3\ mole^{-1} \cdot s^{-1}$. The fact that k^T_{rec} is close in value to k_{rec} implies that very few singlet recombination products are formed in the encounters, i.e., $\kappa_S \ll \kappa_T$. The radicals are assumed to be generated at a distance of 7 Å, at which distance they are also assumed to recombine (this contact distance has been estimated from experimental data[5]). Using the solvent parameters given in Table V, the following values were calculated: $\kappa_S = 4.63$ Å/ns and $\kappa_T = 136$ Å/ns. Using these rates in Eq. (6.3), one obtains the total recombination yields $\phi(\kappa_S) \simeq 20\%$ and $\phi(\kappa_T) \simeq 88\%$. These yields would be achieved at $t \to \infty$ if the pairs would stay all the time in the singlet (triplet) state. Since the hyperfine mechanism changes the electron spin state of the pairs in time (see Fig. 1), the actual (singlet or triplet) yields, as calculated from Eqs. (2.19) and (2.20) and given in Table VI, are smaller.

TABLE VI. Geminate recombination yields of the system $^2Py^{\cdot-} + {}^2DMA^{\cdot+}$ in acetonitrile[a] 50 ns after pair generation.

	Recombination yield in percent	
	$B = 0$	$B \to \infty$
$\phi^{gem}_{S\to S}$	16.3	17.5
$\phi^{gem}_{S\to T}$	12.3	7.2
$\phi^{gem}_{T\to S}$	0.15	0.083
$\phi^{gem}_{T\to T}$	86.6	86.9

[a]$\kappa_S = 4.63$ Å/ns, $\kappa_T = 136$ Å/ns, $T = 25\,^{\circ}C$, $r_1 = 7.0$ Å. Solvent parameters as in Table V; the step lengths employed in the finite-difference method 3 are given below Table I.

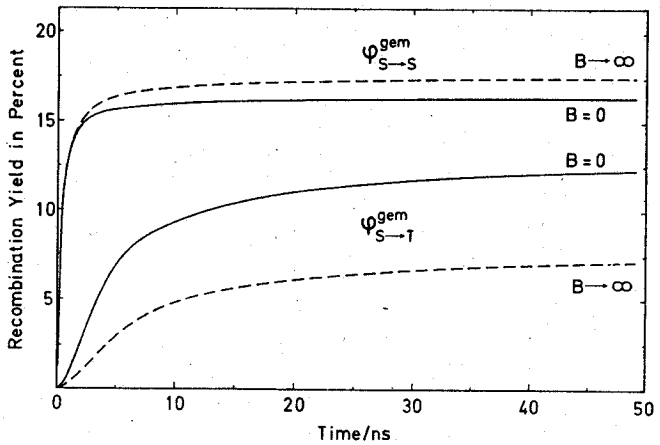

FIG. 5. Time evolution of the singlet and triplet geminate recombination yields at zero and high magnetic field for the system $^2Py^- + {}^2DMA^+$ in acetonitrile (solvent parameters as in Table III, $T = 25\,°C$, $\kappa_S = 4.63$ Å/ns, $\kappa_T = 136$ Å/ns).

The time evolution of the singlet and triplet geminate recombination yields is illustrated in Fig. 5. The singlet recombination yield $\phi^{gem}_{S\to S}(t, B)$ is observed to increase very rapidly, reaching 90% of its saturation value already at about 2 ns. In contrast, the triplet recombination yield $\phi^{gem}_{S\to T}(t, B)$ increases more slowly and reaches 90% of its saturation value after about 20 ns. The initial rise of the geminate triplet recombination yield reflects the time evolution of the hyperfine-induced triplet probability which according to Fig. 1 takes about 5 ns to develop to its maximum value. The initial rise is followed by a long time tail of triplet formation.

Figure 5 and Table VI also demonstrate that an applied magnetic field strongly decreases the geminate triplet recombination yield $\phi^{gem}_{S\to T}$ and increases the geminate singlet recombination yield $\phi^{gem}_{S\to S}$. This behavior is to be expected from the magnetic field dependence of the triplet probability $p^0_T(t)$ of $^2Py^- + {}^2DMA^+$ in Fig. 1. The magnetic field effect, e.g., the difference between the $B = 0$ and $B \to \infty$ triplet yield curves, builds up essentially only within the first few nanoseconds and stays nearly constant from there on.

From the yields in Table VI one can evaluate the *homogeneous* recombination rate constants k_{rec} and k^T_{rec} by virtue of Eqs. (6.5) and (6.6), respectively, for zero and large magnetic fields:

$$k_{rec}(B=0) = 4.20\times10^{10}\ \text{dm}^3\ \text{mole}^{-1}\cdot\text{s}^{-1},$$

$$k_{rec}(B\to\infty) = 4.15\times10^{10}\ \text{dm}^3\ \text{mole}^{-1}\cdot\text{s}^{-1},$$

and

$$k^T_{rec}(B=0) = 3.95\times10^{10}\ \text{dm}^3\ \text{mole}^{-1}\cdot\text{s}^{-1},$$

$$k^T_{rec}(B\to\infty) = 3.89\times10^{10}\ \text{dm}^3\ \text{mole}^{-1}\cdot\text{s}^{-1}.$$

These results demonstrate that in contrast to the geminate recombination, the homogeneous recombination process is practically not influenced by a magnetic field. Note that according to Eq. (6.1) no magnetic field effect on the rate constant k_{rec} is expected for the case $\kappa_S = \kappa_T$. The above results show that also in the case of a rather strong preference of the triplet recombination over the singlet recombination ($\kappa_S \ll \kappa_T$), k_{rec} is altered only by about 1% if a magnetic field is applied.

VII. SOLVENT, TEMPERATURE, CONCENTRATION, ISOTOPE, AND MAGNETIC FIELD EFFECTS ON THE GEMINATE RECOMBINATION OF THE $^2Py^- + {}^2DMA^+$ RADICAL ION PAIR SYSTEM

In the following we wish to investigate the influence of different solvents on the geminate recombination yields. For this purpose we have evaluated the geminate singlet and triplet recombination yields of the system $^2Py^- + {}^2DMA^+$ in typical polar solvents of different polarity and viscosity [acetonitrile (ACN), *N,N*-dimethylformamide (DMF), methanol, ethanol, and propanol, see Table V]. Unfortunately, the homogeneous recombination rate constants k_{rec} and k^T_{rec} needed for the determination of the microscopic rate constants κ_S and κ_T (see Sec. VI) have not been measured yet for the system $^2Py^- + {}^2DMA^+$ in these solvents. At present, we can only estimate the rate constants κ_S and κ_T from the observed magnetic field effect on the triplet and free ion yields.[3] However, as we will demonstrate now for the solvent acetonitrile, one can readily obtain the yields for any other set of κ_S and κ_T values from the diagrams in Fig. 6. The abcissa of Fig. 6 represents the total geminate recombination yield[19] ϕ given by Eq. (6.3) for the κ values plotted in Fig. 6(a). κ increases very fast with increasing ϕ and is infinite for $\phi = 1$. In Fig. 6(b) the behavior of the geminate *triplet* recombination yield for fixed $\hat{\kappa}_S = 18.53$ Å/ns ($\phi = 0.5$) and varied κ_T, and for fixed $\hat{\kappa}_T = 18.53$ Å/ns and varied κ_S is presented. It is observed that the triplet yield increases *linearly* with increasing $\phi(\kappa_T)$ for fixed κ_S but decreases with increasing $\phi(\kappa_S)$ for fixed κ_T.

The latter effect results from the increasing amount of singlet pairs which react at very short times sup-

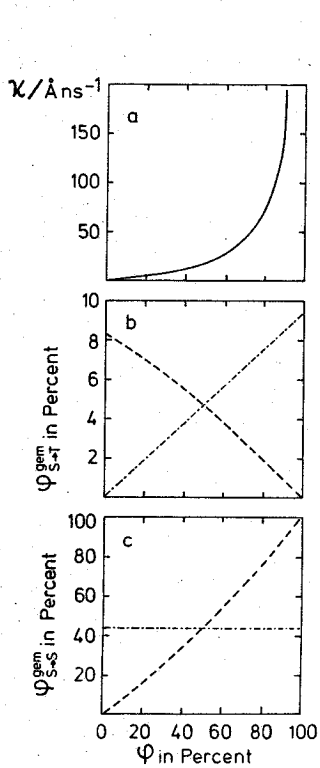

FIG. 6. Influence of the rate constants κ_S and κ_T on the geminate recombination yields in acetonitrile. (a) κ as a function of the total recombination yield[19] defined in Eq. (6.3) for acetonitrile (solvent parameters see Table V). (b) – – –; geminate triplet recombination yield $\phi^{gem}_{S\to T}$ as a function of $\phi(\kappa_S)$, $\hat{\kappa}_T = 18.53$ Å/ns fixed; –·–·–: geminate triplet recombination yield $\phi^{gem}_{S\to T}$ as a function of $\phi(\kappa_T)$, $\hat{\kappa}_S = 18.53$ Å/ns fixed. (c) – – –: geminate singlet recombination yield $\phi^{gem}_{S\to S}$ as a function of $\phi(\kappa_S)$, $\hat{\kappa}_T = 18.53$ Å/ns fixed; –·–·–: geminate singlet recombination yield $\phi^{gem}_{S\to S}$ as a function of $\phi(\kappa_T)$, $\hat{\kappa}_S = 18.53$ Å/ns fixed.

TABLE VII. Solvent effect on $^2Py^- + {}^2DMA^+$ geminate singlet and triplet recombination yields for $\kappa_S = \kappa_T = 18.53$ Å/ns.[a]

Solvent	$\phi_S(B=0)$[b]	$\phi_S(B\to\infty)$	$\phi_T(B=0)$[b]	$\phi_T(B\to\infty)$	$\frac{\phi_T(B\to\infty)}{\phi_T(B=0)}$
ACN	0.437	0.458	0.0468	0.0262	0.560
CH_3OH	0.583	0.610	0.0612	0.0340	0.556
DMF	0.615	0.642	0.0621	0.0346	0.557
C_2H_5OH	0.786	0.815	0.0634	0.0345	0.544
C_3H_7OH	0.904	0.925	0.0454	0.0238	0.524

[a]This κ value corresponds to a total recombination yield in acetonitrile of 50%.

[b]Yields are given at 50 ns after pair generation (see footnote c of Table III), diffusion coefficients and dielectric constants are given in Table V, for the hyperfine coupling constants see text. The radical ion pairs are assumed to be generated at 7 Å, at which distance they are also assumed to recombine. The step lengths employed in the finite difference method 3 are given below Table I.

pressing the amount of triplet pairs formed through the action of the hyperfine mechanism at longer times. The triplet yield for an arbitrary set of κ_S and κ_T values can be obtained by scaling the value $\phi^{gem}_{S-T}(\kappa_S, \hat{\kappa}_T)$ by the factor $\phi^{gem}_{S-T}(\hat{\kappa}_S, \kappa_T)/\phi^{gem}_{S-T}(\hat{\kappa}_S, \hat{\kappa}_T)$. Figure 6(c) shows the corresponding dependence of the geminate *singlet* recombination yield on the κ_S and κ_T values. Owing to the fact that during the geminate phase of the recombination there is on the average almost no singlet production from triplet pairs (see Fig. 1), the singlet yield is found to be nearly independent of κ_T.

In Tables VII, VIII, and IX the yields of singlet and triplet products 50 ns after pair generation are compared for $B=0$ and $B\to\infty$ in various solvents. In order to focus on the solvent effect influencing the recombination yields through the diffusion process, we assumed in our calculations the rate constants κ_S and κ_T to be characteristic for the radical pair system and independent of the solvent. Since the energy gap between the radical ion pair state and the ground state is large, this may be a reasonable assumption for κ_S. The energy gap between the ion pair state and the triplet state $^3Py^* + {}^1DMA$ is much smaller, and therefore κ_T is expected to depend more sensitively on the dielectric relaxation properties of the solvent.[23,24] However, since κ_T is rather large, its variation does not critically influence the recombination yields (see Fig. 6). In Tables VII–IX the same κ_T value (18.53 Å/ns) is used throughout, but in order to demonstrate the sensitivity of the triplet yield and its solvent dependence on κ_S, various κ_S values have been employed in the three tables. As shown above, the triplet yields for other κ_T values can be obtained by multiplication with the factor $\phi(\kappa_T)/\phi(18.53$ Å/ns).

The yield values in Table VII are evaluated for spin-independent geminate recombination, i.e., $\kappa_S = \kappa_T = 18.53$ Å/ns. This value corresponds to the total recombination yields[19] 50.0%, 66.4%, 69.7%, 86.7%, and 96.0% in the solvents ACN, methanol, DMF, ethanol, and propanol, respectively. As expected from these values, the singlet yield $\phi^{gem}_{S-S}(50$ ns, $B)$ in Table VII increases strongly with increasing solvent viscosity and decreasing polarity. This is not the case, however, for the triplet yield $\phi^{gem}_{S-T}(50$ ns, $B)$, which increases in going from acetonitrile to ethanol but decreases again for the solvent propanol. This behavior is readily understood by the competition between singlet and triplet recombination explained above in connection with Fig. 6(b). As has been discussed in Sec. V, the decrease of the triplet yield from ethanol to propanol is predicted to be even more pronounced if an exchange interaction $J(r)$ in the contact region of the radical pair is taken into account.

The solvent effect on the triplet yield should become more distinct for a reduced recombination probability of singlet pairs, i.e., small κ_S. In Table VIII we present the results for the extreme case of no recombination to singlet products ($\kappa_S = 0$). In this case the triplet yield rises from about 5% for acetonitrile to 30% for propanol. A comparison of the results for the solvents acetonitrile and dimethylformamide, of almost identical polarity ($\epsilon = 37.5$ and $\epsilon = 37.6$) but rather different viscosities, shows the considerable influence of the diffusion coefficient D on the triplet recombination yield.

Tables VII and VIII also demonstrate that the free ion yield $\phi_{ion} = 1 - \phi^{gem}_{S-S} - \phi^{gem}_{S-T}$ depends strongly on the value of κ_S. In the case of $\kappa_S = \kappa_T$ presented in Table VII, a free ion yield of only 50% in the solvent acetonitrile, 35% in methanol, 32% in dimethylformamide, and 15% in ethanol is predicted. The experimental observations give, however, larger free ion yields in these solvents,[3] which again is in agreement with our conclusion that κ_S is smaller than κ_T.

In Table IX we present the singlet and triplet yields $\phi^{gem}_{S-S}(50$ ns, $B)$ and $\phi^{gem}_{S-T}(50$ ns, $B)$ for $\kappa_S = 6.176$ Å/ns and $\kappa_T = 18.53$ Å/ns. The κ_S value corresponds to total recombination yields[19] of 25.0%, 39.7%, 43.4%, 68.5%, and 88.8% in the solvents ACN, methanol, DMF, ethanol, and propanol, respectively. In this case the geminate triplet recombination behavior is intermediate to the case of Tables VII and VIII. The triplet yield increases considerably in going from acetonitrile to ethanol but is slightly reduced in propanol. The yields given in Table IX are in reasonable agreement with experimental results.[3]

The solvent influence on the *time-dependent* triplet geminate recombination yields corresponding to Table IX is presented in Fig. 7. Except for scaling factors,

TABLE VIII. Solvent effect on $^2Py^- + {}^2DMA^+$ triplet recombination yield for $\kappa_S = 0$ and $\kappa_T = 18.53$ Å/ns.[a]

Solvent	$\phi_T(B=0)$[b]	$\phi_T(B\to\infty)$	$\frac{\phi_T(B\to\infty)}{\phi_T(B=0)}$	$\frac{\phi_{ion}(B\to\infty)}{\phi_{ion}(B=0)}$
ACN	0.0833	0.0486	0.583	1.038
CH_3OH	0.145	0.0865	0.597	1.068
DMF	0.158	0.0951	0.602	1.075
C_2H_5OH	0.276	0.175	0.634	1.140
C_3H_7OH	0.397	0.269	0.678	1.212

[a]This κ value corresponds to a recombination yield of 50%[19] in acetonitrile.

[b]See Table VII.

TABLE IX. Solvent effect on $^2Py^- + {}^2DMA^+$ geminate singlet and triplet recombination yields for $\kappa_S = 6.176$ Å/ns and $\kappa_T = 18.53$ Å/ns.[a]

Solvent	$\phi_S(B=0)$[b]	$\phi_S(B\to\infty)$	$\phi_T(B=0)$[b]	$\phi_T(B\to\infty)$	$\frac{\phi_T(B\to\infty)}{\phi_T(B=0)}$	$\frac{\phi_{ion}(B\to\infty)}{\phi_{ion}(B=0)}$
ACN	0.206	0.220	0.0664	0.0380	0.573	1.020
CH_3OH	0.317	0.342	0.101	0.0580	0.575	1.031
DMF	0.347	0.374	0.106	0.0611	0.577	1.032
C_2H_5OH	0.547	0.592	0.137	0.0779	0.570	1.044
C_3H_7OH	0.750	0.800	0.122	0.0673	0.550	1.040

[a]These κ values correspond to recombination yields in acetonitrile of 25% (κ_S) and 50% (κ_T), respectively.[19]
[b]See Table VII.

the yield curves of the various solvents appear to be of similar shape. A comparison of the triplet yield curves for ethanol and propanol demonstrates, however, that in the less polar and more viscous solvent propanol the increase of the triplet yield is relatively faster initially owing to the slower separation of the radical pair, but at longer times it is slower. The latter effect results from the competition between the singlet and triplet recombination discussed above.

Tables VII, VIII, and IX show that the relative magnetic field effect on the triplet yield $[\phi^{gem}_{S\to T}(50\text{ ns}, B\to\infty)/\phi^{gem}_{S\to T}(50\text{ ns}, B=0)]$ is insensitive with respect to solvent polarity and viscosity. It depends, however, slightly on the choice of κ_S. The reason for this behavior is that the ratio of hyperfine-induced singlet↔triplet transition probabilities $1 - p^0_T(t, B\to\infty)/p^0_T(t, B=0)$ decreases from an initial value of $\frac{2}{3}$ within the rise time of the triplet probability to a value of about 0.4 at longer times. Consequently, the largest relative lowering of the triplet yield with increasing field strength is achieved if triplet products are formed only at short times, i.e., for large κ_S as in the case presented in Table VII. In the case $\kappa_S = 0$ a considerable fraction of triplet products is formed at longer times and, hence, the relative magnetic field effect is smaller, as demonstrated by Table VIII.

For the case $\kappa_S = \kappa_T = \kappa$ no magnetic field effect on the free ion yield $\phi_{ion} = 1 - \phi^{gem}_{S\to S} - \phi^{gem}_{S\to T}$ can be expected. However, if $\kappa_S \ll \kappa_T$, fewer radical ion pairs will recombine when a field is applied, and hence, there will be a positive magnetic field effect on the free ion yield. This is shown for the extreme case $\kappa_S = 0$ in the last column of Table VIII. The relative magnetic field effect on the free ion yield is strongly influenced by the solvent polarity and viscosity and is found to vary between 4% for acetonitrile and 21% for propanol. The last column of Table IX shows the relative magnetic field effect on the free ion yield for the values $\kappa_S = 6.176$ Å ns^{-1} and $\kappa_T = 18.53$ Å ns^{-1}. In this case the influence of the solvent is much less pronounced and the magnetic field effect on the free ion yield varies only slightly, between 2% and 4% for acetonitrile and propanol, respectively. We note that small positive magnetic field effects on the free ion yield have been observed experimentally.[3] Although the magnetic field effect on the free ion yield is small and, consequently, a rather insensitive quantity, it may be regarded as a measure for the ratio κ_S/κ_T.

Figure 8 compares the magnetic field dependence of $\phi^{gem}_{S\to T}(50\text{ ns}, B)/\phi^{gem}_{S\to T}(50\text{ ns}, B=0)$ for the radical pair system $^2Py^- + {}^2DMA^+$ at low and high donor concentrations (see Sec. III) and for perdeuterated pyrene at high donor concentrations. Curve *a* presents the relative magnetic field effect on the geminate triplet yield of

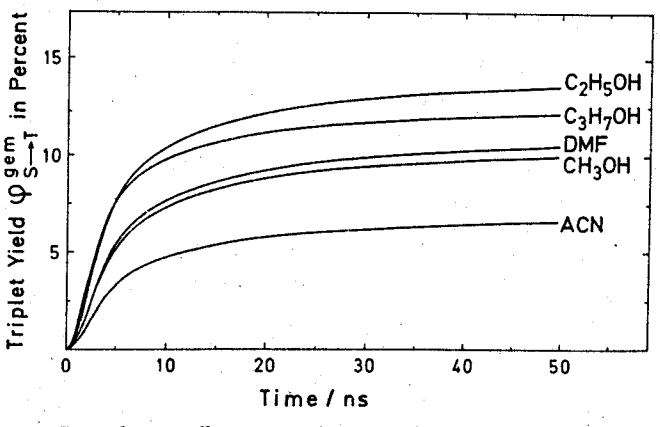

FIG. 7. Solvent influence on the time-dependent triplet recombination yield at zero magnetic field for the system $^2Py^- + {}^2DMA^+$ ($T = 25$ °C, $\kappa_S = 6.176$ Å/ns, $\kappa_T = 18.53$ Å/ns). Solvents: acetonitrile (ACN), *N*,*N*-dimethylformanide (DMF), methanol, ethanol, and propanol characterized through the *D* and ϵ values in Table V.

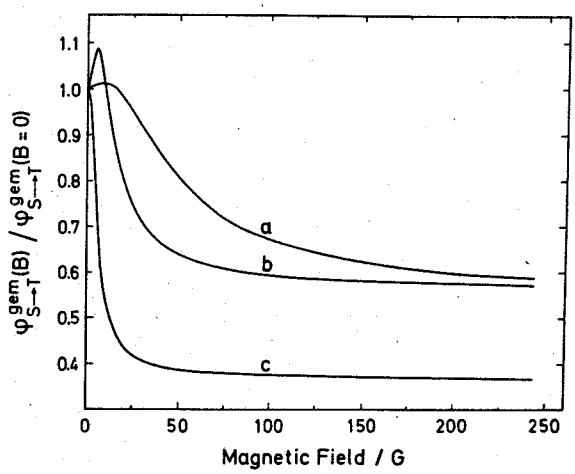

FIG. 8. Magnetic field dependence of the geminate triplet recombination yield in acetonitrile (*D* and ϵ values, see Table V, $T = 25$ °C, $\kappa_S = \kappa_T = 18.53$ Å/ns). (a) $^2Py^- + {}^2DMA^+$; (b) $^2Py^- + {}^2e^+$; (c) $^2d\text{-}Py^- + {}^2e^+$.

TABLE X. Isotope effects on the geminate triplet recombination yields (in %) of $^2Py^- + {}^2DMA^+$ and $^2Py^- + {}^2e^+$ in acetonitrile.[a]

System[b]	ϕ_{S-T}(50 ns, $B=0$)	ϕ_{S-T}(50 ns, $B\to\infty$)
$^2Py^- + {}^2DMA^+$	6.65	3.80
^2d-$Py^- + {}^2d$-DMA^+	...	2.77
$^2Py^- + {}^2e^+$	2.80	1.61
^2d-$Py^- + {}^2e^+$	0.76	0.28

[a]Solvent parameters and rate constants as in Table IX.
[b]See text.

$^2Py^- + {}^2DMA^+$ at low DMA concentrations in acetonitrile (solvent parameters and rate constants as in Table VII). The field effect, as already pointed out above, does not depend sensitively on the solvent parameters and recombination rate constants κ_S and κ_T, but is characteristic of the hyperfine coupling in the recombining radical pair. The excellent agreement between the predicted magnetic field dependence of the triplet yield for the system pyrene–3,5-dimethoxy-*N*,*N*-dimethylaniline and the experimental observation[2] can therefore be considered a direct proof for the hyperfine mechanism to be responsible for the geminate recombination to triplet products.

At high donor (DMA) concentrations, the possibility of a fast electron exchange reaction as discussed in Sec. III exists. Curve *b* in Fig. 8 shows the calculated magnetic field dependence of the system $^2Py^- + {}^2e^+$ describing the extreme situation that there is no effective hyperfine coupling in the DMA^+ radical ions. The solvent is again acetonitrile with the parameters in Table VII. As the hyperfine coupling in this system is much weaker than in $^2Py^- + {}^2DMA^+$, smaller field strengths suffice to suppress the $S \leftrightarrow T_{\pm 1}$ transitions and, thus, to lower the triplet yield. The existence of electron exchange reactions, therefore, could be verified by the experimental observation of a concentration dependence in the magnetic field effect. The magnetic field effect on the system ^2d-$Py^- + {}^2e^+$ (perdeuterated pyrene at high donor concentrations) is depicted by curve *c* in Fig. 8. As in this case the hyperfine coupling is very weak owing to the small hyperfine coupling constants of the deuterium spins, magnetic fields of just a few gauss induce a strong percentile reduction of the geminate triplet yield (the absolute yield being small, however).

Curves *a* and *b* in Fig. 8 show $\phi^{gem}_{S-T}(50\text{ ns}, B)/\phi^{gem}_{S-T}(50\text{ ns}, B=0)$ to increase at low fields by about 1% and 8%, respectively. This increase originates from the fact that at low magnetic fields B the triplet probability $p^0_T(t, B)$ is very close in value to $p^0_T(t, B=0)$ during the initial rise but exceeds $p^0_T(t, B=0)$ at later times (see Figs. 1 and 2). The increase of $\phi^{gem}_{S-T}(50\text{ ns}, B)/\phi^{gem}_{S-T}(50\text{ ns}, B=0)$ above the value 1 is hence due to triplet recombination products in the time span between about 5 ns and 14 ns for the system $^2Py^- + {}^2DMA^+$ and for times longer than ~ 15 ns for the system $^2Py^- + {}^2e^+$.

The different time evolution of the triplet probability $p^0_T(t)$ for systems characterized by different hyperfine coupling situations leads also to very different geminate triplet recombination yields. In Table X the triplet yields of the nondeuterated and deuterated radical pair system $^2Py^- + {}^2DMA^+$ and $^2Py^- + {}^2e^+$ in acetonitrile are compared. In all cases the recombination rate constants were chosen to be $\kappa_S = 6.176$ Å ns^{-1} and $\kappa_T = 18.53$ Å ns^{-1} disregarding any possible isotope effect on the electron transfer process. As is to be expected, the largest triplet yield is predicted for $^2Py^- + {}^2DMA^+$ with the largest hyperfine coupling constants. At high magnetic fields the triplet yield is lowered by about 1% if pyrene and DMA are perdeuterated (compare Fig. 3), a value which may be modified by a possible isotope effect on the rate constants κ_S and κ_T. Under the assumption that at high donor concentrations only the nuclear spins on the pyrene radical contribute to the hyperfine induced singlet↔triplet transition, the formation of triplet radical pairs is slowed down considerably (compare Figs. 1 and 2). Table X predicts the triplet yield to be reduced then by more than 50%. The triplet yield is predicted to become even smaller, in fact almost negligible, when the pyrene is perdeuterated. In the calculations of Table X, we neglected any increase of the effective relative diffusion coefficient through the greater mobility of a radical electron hopping between the donor molecules. Such an effect would lead to a further reduction of the geminate triplet yields at high donor concentrations.

The temperature dependence of the geminate recombination yields for the system $^2Py^- + {}^2DMA^+$ in methanol is shown graphically in Fig. 9. It results from the combined effects of the temperature dependence of the diffusion coefficient D, the dielectric constant ϵ, and the friction term βF in the Smoluchowski operator (2.3): with increasing temperature D increases, ϵ decreases, and β decreases. We have assumed the rate constants $\kappa_S = 6.176$ Å ns^{-1} and $\kappa_T = 18.53$ Å ns^{-1} to be independent of the temperature, an assumption which may be somewhat unrealistic. Figure 9 demonstrates that the singlet yield is much more sensitive against temperature

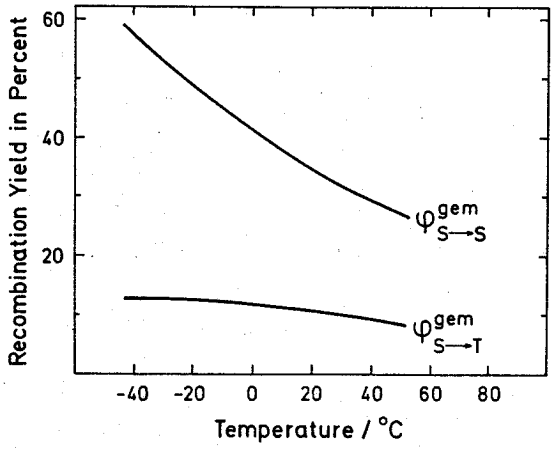

FIG. 9. Temperature dependence of the geminate singlet and triplet recombination yields of the system $^2Py^- + {}^2DMA^+$ in methanol (D and ϵ values, see Table V, $\kappa_S = 6.176$ Å/ns, $\kappa_T = 18.53$ Å/ns). The temperature dependence of the diffusion constant D was evaluated according to $D(t) = D(25\,^\circ\text{C}) \times (T + 273.16/298.16)\,[\eta(25\,^\circ\text{C})/\eta(T)]$. The viscosities $\eta(T)$ and the dielectric constants $\epsilon(T)$ were taken from Ref. 22.

variation than the triplet yield. This may be explained again by the competition between the singlet product formation in the first few nanoseconds and the hyperfine-induced triplet product formation at later times. The difference in the temperature dependence of the triplet and the free ion yield is in qualitative agreement with experimental results.[5]

The theoretical predictions of the time-dependent geminate recombination yields presented above cannot be compared directly with experimental observations. The main reason is that the radical ion pairs are not generated instantaneously, but rather originate from a series of sequential processes started by a laser pulse with a half-width of about 8 ns. In addition there exist competing mechanisms for triplet product formation, for example intersystem crossing in an exciplex preceding the ion pair formation.

In order to account for all these processes one may evaluate the radical ion pair formation rate $R(t)$ [see Eq. (2.1)] by solving the differential equations describing the processes preceding the formation of the radical ion pair. This has been discussed in detail in Ref. 2. Provided the bimolecular rate constants k_{rec} and k_{rec}^T are known from experiment, all parameters entering in the theoretical simulation of the triplet and free ion extinction curves (e.g., initial concentration, rate constants, and extinction coefficients) are either experimentally known or may be fitted unambiguously.[2] This renders possible a direct comparison between the experimental and theoretical magnetic field effect on the triplet yield, which has been shown to be a direct measure of the *geminate* triplet yield. The results of such simulations will be presented together with experimental results elsewhere.

VIII. SUMMARY

We have provided a quantitative theoretical description for the experimentally observed magnetic field modulation of the geminate recombination of radical ion pairs. In the case of different recombination probabilities for the singlet and triplet pairs, the stochastic Liouville equation describing the entire recombination process comprises a large set of coupled diffusion equations. A numerical algorithm has been presented which renders possible the exact solution of the Liouville equation for the spin motion of radical pair systems with only a few nuclear spins in the case of arbitrary magnetic fields as well as for large nuclear spin systems in the high-field case. In order to treat large spin systems at arbitrary magnetic fields, we have introduced an approximate Liouville equation entailing only two coupled diffusion equations. This simple approximation has been demonstrated to yield results in excellent agreement with the exact results available.

The principal conclusions derived from our study are the following: The triplet geminate recombination yield depends sensitively on the strength of the hyperfine coupling in the radical ions and is lowered by more than 40% when an external magnetic field is applied. The magnetic field effect on the homogeneous recombination is negligible. Applying the theory to the system $^2Py^- + {}^2DMA^+$, we investigated the solvent and temperature dependence of the geminate recombination yields. As expected, the singlet yield was found to increase strongly with decreasing solvent polarity, increasing viscosity, and decreasing temperature. However, this is not so for the geminate triplet recombination yield, which is much less influenced by the solvent. This result can be explained by the competition between singlet recombination, occurring shortly after pair generation, and the triplet recombination, starting only after the hyperfine mechanism has succeeded to convert the radical pair from the singlet to the triplet electron spin state.

In the calculations mentioned so far, the exchange interaction $J(r)$ (singlet–triplet splitting) in the contact region of the radical pairs had been neglected. Its influence on the geminate recombination yield has been studied in Sec. V. Since the exchange in interaction suppresses the singlet↔triplet transition probability, it also reduces the geminate triplet yield. This effect has been shown to be important only in the case of weakly polar solvents.

Our description of the geminate radical ion pair recombination process has been based on the macroscopic system properties, e.g., solvent viscosity and dielectric constant. So far, little is known about these properties on the microscopic scale for radical pair separations comparable with molecular dimensions. Furthermore, for lack of information concerning anisotropic reaction propensities, we have assumed the diffusion and recombination processes to be spherically symmetric. We hope that our work will stimulate more experimental investigations of geminate radical reactions from which information about the microscopic details of the diffusion as well as the recombination processes can be abstracted.

ACKNOWLEDGMENTS

We wish to thank Professor Albert Weller for his support, important suggestions, and more so for having introduced us to the radical reactions considered in this paper. We thank Hubert Staerk for many useful discussions and also acknowledge the use of the excellent computer facilities of the Gesellschaft für wissenschaftliche Datenverarbeitung mbH Göttingen.

APPENDIX: STATISTICAL TREATMENT OF HYPERFINE COUPLING INDUCED SINGLET →TRIPLET TRANSITIONS AT LARGE MAGNETIC FIELDS

At large magnetic fields and for $g_1 = g_2$ the Hamiltonian (2) couples only the S_0 and T_0 electron spin states. In this limit the triplet probability $p_T^0(t)$ defined as in Sec. II can be evaluated analytically. For radical pairs with n nuclear spins $\frac{1}{2}$ and hyperfine coupling constants a_i, $i = 1, \ldots n$,

$$p_T^0(t) = \frac{1}{2^n} \sum_N \sin^2 \frac{a(N)}{4} t \,, \tag{A1}$$

where the summation goes over all 2^n nuclear spin states N and

$$a(N) = 2\sum_i a_i m_i \quad (m_i = \pm 1/2)\,. \tag{A2}$$

Brocklehurst[9] has simplified the expression (A1),

$$p_T^0(t) = \frac{1}{2}\left(1 - \prod_{i=1}^{n} \cos\frac{a_i}{2}\,t\right)\,. \tag{A3}$$

From this expression it is not evident why $p_T^0(t)$ at large fields, as illustrated in Figs. 1 and 2, assumes such a simple functional behavior, a sigmoidal increase from zero to the value $\frac{1}{2}$. Rather, from the expressions (A1) and (A3) which depend on n parameters a_i, one may expect a more complicated functional behavior. We will show now that, in fact, $p_T^0(t)$ can be approximated by

$$p_T^0(t) = \frac{1}{2}\left\{1 - \exp\left[-\frac{1}{8n}\left(\sum_i |a_i|\right)^2 t^2\right]\right\}, \tag{A4}$$

an expression which depends solely on the sum of hyperfine coupling constants $\sum_i |a_i|$ and on n, and which reflects directly the sigmoidal behavior of $p_T^0(t)$.

To obtain (A4) we replace in (A2) the hyperfine coupling constants a_i by their average value

$$\langle a\rangle = \frac{1}{n}\sum_i |a_i|\,. \tag{A5}$$

$a(N)$ assumes then the values $2k\langle a\rangle$, $k = -n/2,\ -n/2+1, \ldots, n/2$ for

$$\binom{n}{\frac{1}{2}n + k}$$

nuclear configurations. The validity of approximation (A4) depends on how accurately the distribution (A2) of the $a(N)$ values is described by this binomial distribution. The replacement (A5) simplifies (A1):

$$p_T^0(t) \simeq \frac{1}{2^n} \sum_{k=-n/2,-n/2+1,\ldots}^{n/2} \binom{n}{\frac{1}{2}n + k} \sin^2 k\,\frac{\langle a\rangle}{2}\,t\,. \tag{A6}$$

As[25]

$$(1/2)^n \binom{n}{\frac{n}{2} + k} \simeq 2(2\pi n)^{-1/2} \exp(-2k^2/n)\,,$$

this sum may be replaced by the integral

$$p_T^0(t) \simeq \int_{-\infty}^{\infty} \frac{2}{\sqrt{2\pi n}} \exp(-2x^2/n) \sin^2 x\,\frac{\langle a\rangle}{2}\,t\,. \tag{A7}$$

This integral can be evaluated, and with the definition (A5) for $\langle a\rangle$ one obtains the expression (A4). The replacement of (A6) by (A7) involves the "short time approximation" which holds for $\langle a\rangle t \ll 1$.

[1] *Chemically Induced Magnetic Polarization*, edited by A. R. Lepley and G. L. Closs (Wiley, New York, 1973).

[2] K. Schulten, H. Staerk, A. Weller, H.-J. Werner, and B. Nickel, Z. Phys. Chem. **NF101**, 371 (1976).

[3] H.-J. Werner, H. Staerk, and A. Weller (to be published).

[4] H. Leonhard and A. Weller, Z. Phys. Chem. **NF29**, 277 (1961).

[5] H. Schomburg, dissertation, Göttingen, 1975.

[6] H. Schomburg, H. Staerk, and A. Weller, Chem. Phys. Lett. 21, 433 (1973); 22, 1 (1973).

[7] N. Orbach and M. Ottolenghi, in *The Exciplex*, edited by M. Gordon and W. R. Ware (Academic, New York, 1975), p. 75.

[8] R. P. Groff, R. E. Merrifield, A. Suna, and P. Avakian, Phys. Rev. Lett. 29, 429 (1972); R. P. Groff, A. Suna, P. Avakian, and R. E. Merrifield, Phys. Rev. B 9, 2655 (1974).

[9] B. Brocklehurst, J. Chem. Soc. Faraday Trans II 72 1869 (1976); Chem. Phys. Lett. 28, 357 (1974); Nature 221, 221, 921 (1969).

[10] M. E. Michel-Beyerle, R. Haberkorn, W. Bube, E. Steffens, H. Schröder, H. J. Neusser, E. W. Schlag, and H. Seidlitz, Chem. Phys. 17, 139 (1976).

[11] Z. Schulten and K. Schulten, J. Chem. Phys. 66, 4676 (1977).

[12] See, for example, E. P. Wigner, *Group Theory and Its Application to the Quantum Mechanics of Atomic Spectra* (Academic, London, 1959).

[13] H. W. Brown and R. C. Jones, J. Chem. Phys. 36, 2809 (1962).

[14] B. M. Latta and R. W. Taft, J. Am. Chem. Soc. 89, 5172 (1967).

[15] This possibility has been suggested to us by A. Weller.

[16] See, for example, A. Carrington and A. D. McLachlan, *Introduction to Magnetic Resonance* (Harper and Row, New York, 1967), p. 2.

[17] (a) J. B. Pedersen and J. H. Freed, J. Chem. Phys. 58, 2746 (1973); (b) *ibid.* 59, 2869 (1973); (c) A review of this work is found in J. H. Freed and J. B. Pedersen, Adv. Magn. Reson. 8, 1–84 (1976).

[18] (a) R. D. Richtmeyer and K. W. Morton, *Difference Methods for Initial-Value Problems* (Wiley-Interscience, New York, 1967), p. 189; (b) *ibid.*, p. 198.

[19] These singlet (triplet) yields are evaluated from Eq. (6.3). They would be achieved at $t \to \infty$ if the pairs would stay all the time in the singlet (triplet) state.

[20] I. Amdur and G. G. Hammes, *Chemical Kinetics: Principles and Selected Topics* (McGraw-Hill, New York, 1966), p. 59; This expression has also been discused in Ref. 11 and Ref. 17(c). The rate constant κ used in Ref. 11 and this paper is related to Pedersen and Freed's first-order rate constant k for the back electron transfer by $k = 2\kappa/h_1$, where h_1 is the width of the annular contact region.

[21] The diffusion coefficients in acetonitrile at 25 °C $D_{Py}^{25} = 2.07 \times 10^{-5}$ cm^2 s^{-1} and $D_{DMA}^{25} = 2.46 \times 10^{-5}$ cm^2 s^{-1} have been obtained from a nomogram of D. F. Othmer and M. S. Thaker, Ind. Eng. Chem. 45, 589 (1953) by a procedure outlined by D. Rehm and A. Weller, Ber. Bunsenges. Phys. Chem. 73, 834 (1969). The values in the other solvents were obtained according to Walden's rule $D_x^{25} = D_{ACN}^{25}\,(\eta_{ACN}^{25}/\eta_x^{25})$, the viscosities η taken from Ref. 22. Since the diffusion coefficients have not been measured for the radical ions, the above values for the neutral molecules have been taken.

[22] Landolt-Börnstein, *Zahlenwerte und Funktionen*, 6. Aufl., II. Band, 5. Teil (Springer, Berlin, 1969), and 6. Teil (Springer, Berlin, 1959).

[23] R. A. Marcus, J Chem. Phys. 43, 2654 (1965); 52, 2803 (1970).

[24] G. Ramunni and L. Salem, Z. Phys. Chem. **NF 101**, 123 (1976).

[25] W. Feller, *An Introduction to Probability: Theory and Its Application* (Wiley, New York, 1968), 3rd ed., Vol. I, Chap. 7.